Technical University of Denmark

DTU

A preliminary assessment of potential doses to man from radioactive waste dumped in the Arctic sea

Nielsen, Sven Poul; Iosjpe, M.; Strand, P.

Publication date:
1995

Document Version
Publisher's PDF, also known as Version of record

Link back to DTU Orbit

DTU Library
Technical Information Center of Denmark

A Preliminary Assessment of Potential Doses to Man from Radioactive Waste Dumped in the Arctic Sea

Sven P. Nielsen, Mikhail Iosjpe * and Per Strand *

* Norwegian Radiation Protection Authority, Østerås, Norway

A Preliminary Assessment of Potential Doses to Man from Radioactive Waste Dumped in the Arctic Sea

Sven P. Nielsen, Mikhail Iosjpe[*] and Per Strand[*]

[*]Norwegian Radiation Protection Authority, Østerås, Norway

Abstract This report describes a preliminary radiological assessment of collective doses to the world population from radioactive material dumped in the Barents and Kara Seas in the period 1961-1991. Information on the dumped waste and the rates of release of radionuclides have been available from Russian sources and from the International Atomic Energy Agency. A box model has been used to simulate the dispersion of radionuclides in the marine environment and to calculate the contamination of seafood and the subsequent radiation doses to man. Two release scenarios have been adopted. The worst-case release scenario which ignores the presence of barriers between spent nuclear fuel and seawater is estimated to give rise to about 10 mansieverts calculated to 1000 years from the time of release. A more realistic release scenario is estimated to cause about 3 mansieverts. In both cases exposure from the radionuclide ^{137}Cs is found to dominate the doses.

CONTENTS

1. INTRODUCTION

Information on disposal of radioactive waste in the shallow waters of the Arctic Seas by the former Soviet Union became first available to the international community from unofficial sources in 1990 and later from official Russian sources in 1993 (White Book No. 3, 1993). Since then several initiatives have been taken to assess the potential impact to man and the environment from this waste. The dumpings have taken place in the Barents Sea west of Novaya Zemlya and in the Kara Sea east of Novaya Zemlya and have covered the period 1960-1991.

The countries bordering the Arctic Seas are particularly concerned in connection with the possible contamination of their harvest of marine produce from these waters. Norway and the Russian Federation have entered into close co-operation to investigate the present levels of artificial radionuclides in the environment near the sites where solid reactor waste and spent nuclear fuel have been dumped in the Kara Sea. The International Atomic Energy Agency (IAEA) launched in 1993 a programme "International Arctic Seas Assessment Project (IASAP)" which is planned to last for four years. The programme is organised by IAEA in co-operation with Norway and Russia.

Risø National Laboratory is working together with IAEA and the Norwegian Radiation Protection Authority in the investigations by carrying out radioanalytical work on environmental samples collected from the joint Norwegian-Russian expeditions (1992, 1993 and 1994) to the Kara Sea and by making a preliminary assessment of the potential collective doses to man from ingestion of seafood contaminated from the waste. The present work has been done in association with the Joint Russian-Norwegian Expert Group for Investigation of Radioactive contamination in the Northern Areas.

2. MODEL

2.1. MODEL DESCRIPTION

The present work is based on box-model analysis used to simulate the movement of radioactive material between the different boxes into which the relevant parts of the environment is subdivided.

Box-model analysis assumes instantaneous uniform mixing within each box with rates of transfer being proportional to the inventories of material in the source boxes. More detailed modelling of water transport is possible with complex (e.g. 3 dimensional) models which may give excellent results at short distances and time scales (Breton and Salomon 1995; Schönfeld 1995). But in connection with radiological assessments of discharges to the marine environment it is often necessary to cover large distances (>1000 km) and long time scales (centuries or millenniums) which may not justify the use of the more complex models neither in terms of cost nor accuracy of the results.
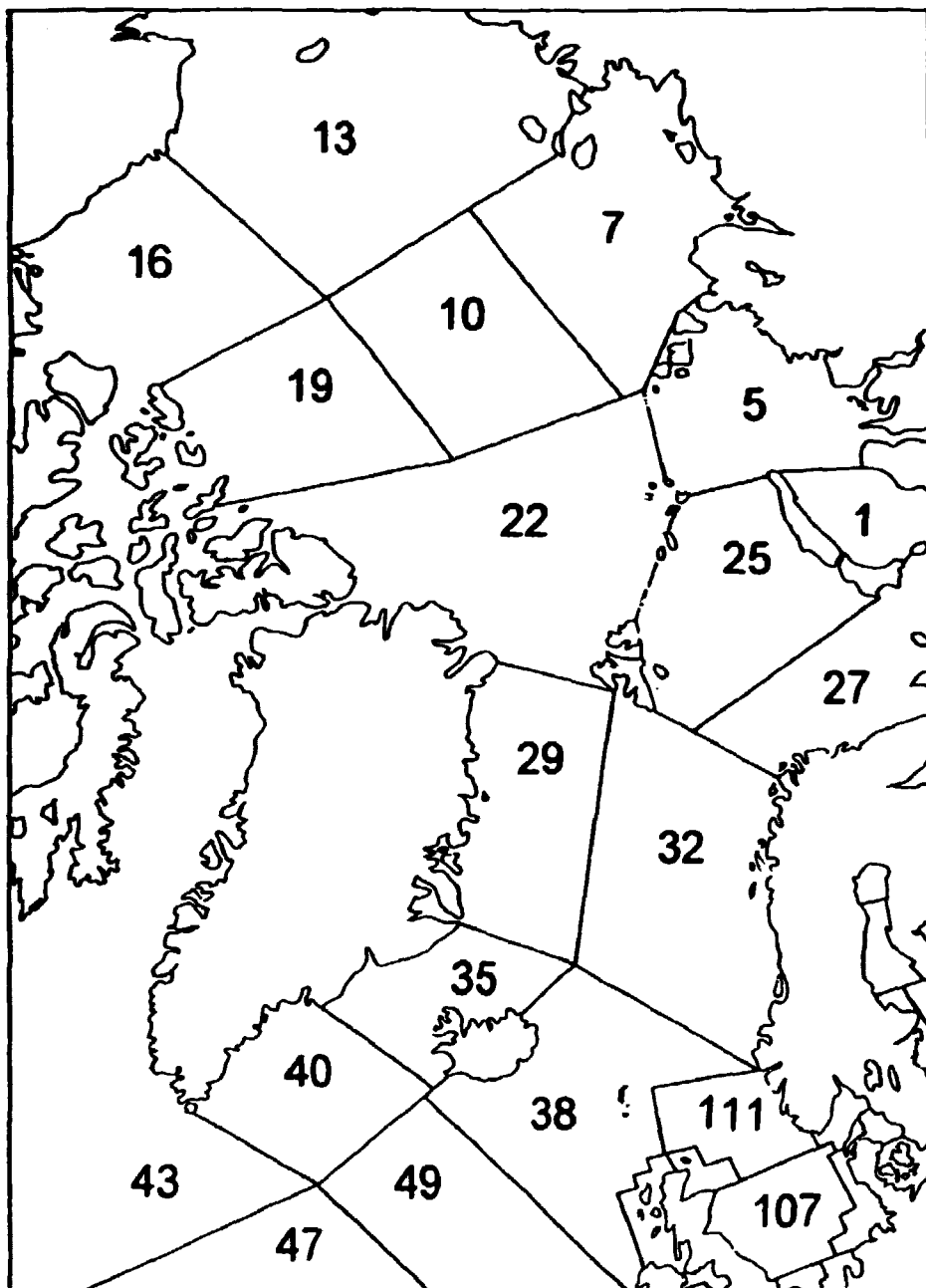
Figure 1. Regions in the Arctic Ocean covered by the box model. The numbers refer to surface water boxes.

Box models have been used previously in connection with studies of the dispersion of discharges of radioactivity from European civil nuclear installations (NRPB and CEA 1979; Camplin et al. 1982; Hallstadius et al. 1987; Nielsen and Aarkrog 1988; CEC 1990). The present model is a combination of two models: 1) the one is an adjusted version (Nielsen 1995) of a regional box model used for radiological assessments in north-west European coastal areas (EC 1995), and 2) the other is a larger box model covering the Arctic Ocean and the North Atlantic (Chartier 1993). The larger box model is derived from a 3D World Ocean general circulation model from which the

results have been used for the design of a box structure in the Arctic Ocean and surrounding waters. The resulting structure and water fluxes were selected taking into account expert information based on experimental data from the Barents Sea (Ådlandsvik 1993).
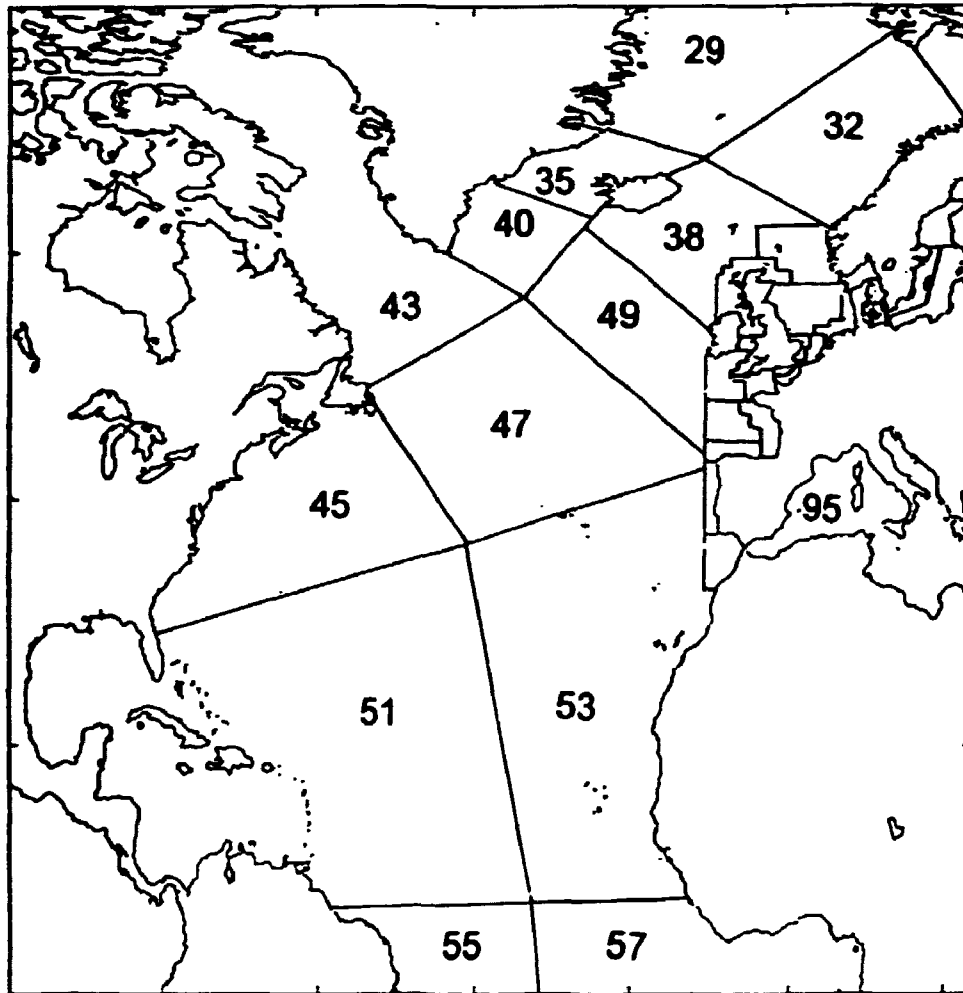

Figure 2. Regions in the North Atlantic covered by the box model. The numbers refer to surface water boxes.

The box-model analysis uses first order differential equations to describe the transfer of pollutants between the boxes. The equations are of the form:

$$\frac{dA_i}{dt} = \sum_{j=1}^{n} k_{ji} A_j - \sum_{j=1}^{n} k_{ij} A_i - k_i A_i + Q_i,$$

where $k_{ii}=0$ for all i, A_i and A_j are activities (Bq) at time t in boxes i and j, k_{ij} and k_{ji} are rates of transfer (y^{-1}) between boxes i and j, k_i is an effective rate of transfer of activity (y^{-1}) from box i taking into account loss of material from the compartment without transfer to another, for example radioactive decay, Q_i is a continuous source of input into box i (Bq y^{-1}) and n is the number of boxes in the system.

The rates of transfer between the aquatic boxes, k_{ij} (y^{-1}) are related to the volume exchanges, R_{ij} (km^3 y^{-1}) according to:

$$R_{ij} = k_{ij}V_i,$$

where V_i is the volume of water represented by box i

Figures 1 and 2 show the regions used in the marine box model and Figure 3 shows the structure of the water boxes and their interconnections. Each of the water compartments has associated suspended sediment and the water compartments in contact with the seabed have underlying seabed sediment compartments. The latter are not shown in Figure 3.
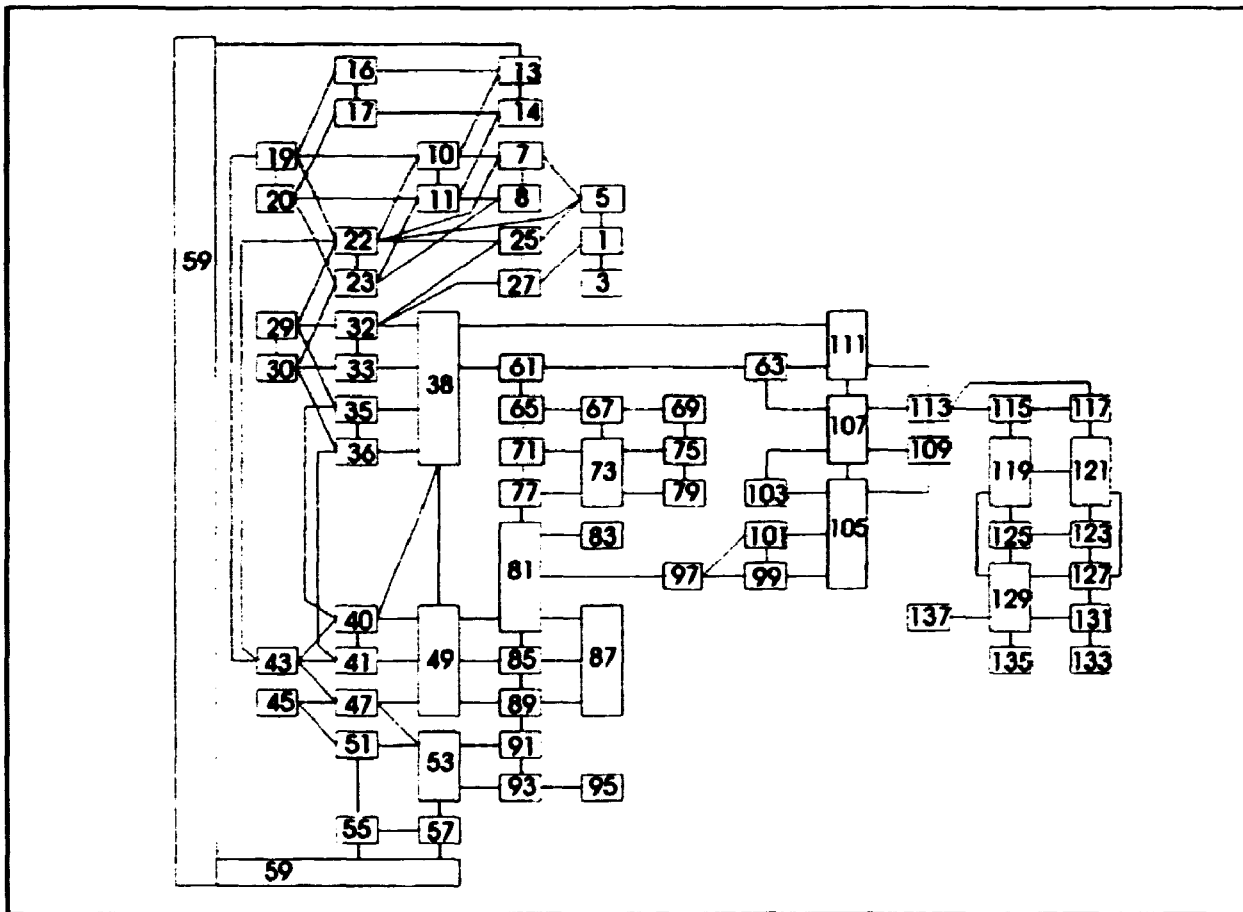
Figure 3. Schematic box structure of the model showing the water boxes only. The lines connecting the boxes indicate the water fluxes between adjacent boxes.

The compartment names, volumes, mean depths, suspended sediment loads and sedimentation rates are given in the Appendix A in Table A1. The volume exchange rates used in the model are given in Table A2. The suspended sediment loads and sedimentation rates are default values based on values from the regional model mentioned above (EC 1995).

At any given time the activity in the water column is partitioned between the water phase and the suspended sediment material. The fraction of the activity (F_w) in the water column which is in solution is given by:

$$F_w = \frac{1}{1 + K_d SSL}$$

where K_d is the sediment distribution coefficient (or concentration factor) ($m^3 \, t^{-1}$) and SSL the suspended sediment load ($t \, m^{-3}$). Activity on suspended sediments is lost to the underlying boxes when particulates settle out. The fractional transfer from a water column (box i) to the sediments (box j) due to sedimentation is given by:

$$k_{ij} = \frac{K_d SR}{d_i (1 + K_d SSL_i)},$$

where d_i (m) is the mean water depth of the water column and SR ($t \, m^{-2} \, y^{-1}$) the mass sedimentation rate.

Resuspension of sediment material including radioactivity from the surface sediment layer to the water column is included in the model to account for the higher suspended sediment loads in shallow coastal regions. Resuspension is considered within each region and is caused mainly by wind and tidal forcing. The model also includes the transfers of radioactivity between the surface sediment layer and the bottom boundary layer comprising diffusivity through the pore water using a diffusion coefficient of $1 \cdot 10^{-9} \, m^2 \, s^{-1}$ and mixing due to bioturbation modelled as a diffusive process using a diffusion coefficient of $1 \cdot 10^{-12} \, m^2 \, s^{-1}$ (EC 1995). Furthermore, removal of activity from the top surface sediment to lower sediment layers is taken into account by assuming that the burial rate is equal to the flux of particles which settle from the overlying waters. Radioactive decay is included in all the boxes.

The dispersion of radioactive material in the marine environment is modelled from the description given above. The contamination of fish, crustaceans and molluscs is further calculated from the radionuclide concentrations in filtered seawater in the different water regions. For this purpose concentration factors for biological material are used. This factor is dimensionless and gives the ratio of the radionuclide concentration in the biological material to that in filtered seawater. Values from the Marina study (CEC 1990) have been used and are shown in the Appendix A in Table A3 which gives for the different radionuclides studied, the halflives, the K_d's, the concentration factors for fish, crustaceans and molluscs, and the dose factors for ingestion.

Data for the catch of seafood in the various regions have been compiled from the Marina study (CEC 1990) supplied with information obtained from the MARDOS project (IAEA 1994) which has dealt with a global assessment of doses to man from radioactivity in the marine environment. The following assumptions (CEC 1990) for the edible fractions of marine produce to the human diet are used: 50% for fish, 35% for crustacea and 15% for molluscs. The quantities of marine produce used for the calculations are shown in the Appendix A in Table A4. The total intakes of activity by man are converted to collective doses by multiplication with the appropriate factors for dose per unit intake.

2.2. MODEL RELIABILITY

The reliability of model predictions is a key issue in connection with all kinds of forecast based on modelling. The reliability of the results from the present model is commented on three points. One point refers to a comparison made between observations and model calculations of seawater concentrations of radioactive tracers. The second point compares collective doses calculated with two different models, and the third point concerns the quality of the basic data used to build the model.

The regional box model which covers the north-west European coastal areas and forms part of the present model, was used for a comparison with observed concentrations of radionuclides in seawater (Nielsen 1995). The radionuclides are ^{137}Cs, ^{99}Tc and ^{125}Sb discharged from the two European reprocessing plants: Sellafield in the United Kingdom and La Hague in France. The comparison between observations and predictions resulted in adjustments of the model with respect to the mixing conditions in the English Channel and North Sea in addition to the water transport from the North Sea to the Baltic Sea. An analysis of the predicted-to-observed seawater concentrations indicated an overall predictive accuracy of 0.9 corresponding to a 10% underestimation and a predictive precision of about a factor of 2.5 at a confidence level of 95%. The ^{125}Sb data were not used for the model adjustments and these data support the general conclusions about the model predictions of radionuclide concentrations in the seawater.

The present model has been used with inputs of ^{137}Cs covering fallout from tests of nuclear weapons in the atmosphere, fallout from the Chernobyl accident in 1986 and routine discharges from the two reprocessing plants, Sellafield and La Hague. The results of these calculations are shown in Table 1 which for comparison shows corresponding numbers from the CEC Marina project. It is important to note that there are significant differences between the assumptions behind the two sets of results. The Marina study involved a large number of radionuclides in addition to ^{137}Cs, other exposure pathways than that of ingestion, and considered only doses to members of the European Community. However, in the Marina study ^{137}Cs was found to be the most important radionuclide by contributing about 40% of the collective dose, and ingestion of fish was found to be the most important exposure pathway. It is therefore of interest to make a rough comparison between the two sets of results, and this comparison does not indicate significant differences between the results.

Table 1. Collective doses calculated with the present model (^{137}Cs only) compared with results from the Marina study (CEC 1990).

Source	Collective dose to year 2500 (manSv)	
	This study (^{137}Cs only)	Marina study
Reprocessing plants	2100	2200
Weapons test fallout	1900	1600
Chernobyl fallout	840	1000

The third point is related to the quality of the 3D World Ocean Circulation Model (Marti 1992) which was used to derive the structure and water fluxes for the box model. The World Ocean model has been used to calculate the dispersion of a number

of tracers with the simulated steady-state circulation and compared with *in situ* data. The agreement was satisfying and the limited discrepancies were explained (Chartier 1993), so this model is considered useful for the calculation of long-range dispersion of conservative or semi-conservative tracers and to provide any water mass fluxes in the World Ocean. A number of items have been considered for the design of the structure of the box model (e.g. time scale of the problem, ICES fishing areas, local marine hydrodynamics, vertical gradients), and data on the water mass fluxes between adjacent boxes have been extracted from the World Ocean Circulation Model. Following expert review (Ådlandsvik 1993) of the fluxes given by the World Ocean circulation Model, modifications have been made to take into account *in situ* observations of currents in the Arctic Ocean. The reliability of the resulting box model thus derived has not been quantified except for areas far from the Arctic Ocean, but qualitatively it can be stated that the box model is based on up-to-date expertise.

3. SOURCE TERMS

The source terms considered have been selected on the basis of information from the White Book No. 3 (1993) and on information from the Source Term Group from the IASAP project previously mentioned. The White Book gives little radionuclide-specific information and presents the amounts of solid reactor waste dumped in terms of ^{90}Sr-equivalent activity in curies. The report specifies the liquid radioactive waste discharged at sea in terms of total activity only, and this is also the case for the almost all dumpings of spent nuclear fuel.

It has here been assumed that radioactivity in liquid and solid reactor waste (LRW and SRW) is dominated by the four radionuclides: ^{3}H, ^{60}Co, ^{90}Sr and ^{137}Cs, and that they occur in equal amounts of activity at the time of dumping or discharge. For spent nuclear fuel (SNF), information has been obtained from the IASAP Source Term Group who are estimating radionuclide-specific release rates from the dumped reactor compartments (including ^{3}H, ^{60}Co, ^{63}Ni, ^{90}Sr, ^{129}I, ^{137}Cs, ^{239}Pu and ^{241}Am).

The White Book gives detailed information on the geographical locations of the discharges of liquid reactor waste and of the dumpings of solid reactor waste and spent nuclear fuel. The use of that information in the present assessment has been limited to the spatial resolution of the present model. However for the spent nuclear waste dumped in the fjords on the east coast of Novaya Zemlya, a generic model fjord was used to simulate the receiving environment before exchange with the Western Kara Sea. The fjord was considered having a volume of 0.5 km^3, an average depth of 20 m and an exchange rate with the Kara Sea of 1 km^3 y^{-1}. The LRW and SRW discharges have thus been assumed to occur directly into either the Western Kara Sea (box 1) or the Barents Sea (box 25 and 27) while the SNF discharges have been assumed to occur either into the fjord or the trough of the Kara Sea (box 3). The limited spatial resolution of the model reduces the potential for making a detailed local assessment, but not for a regional or global assessment.

3.1. UNIT RELEASES

The assessment is based on separate calculations for each radionuclide (*no decay chains are considered*). Therefore, a series of calculations were made based on instantaneous releases of one terabecquerel (TBq = 10^{12} Bq) of each of the eight above mentioned radionuclides in soluble form into a fjord on the east coast of Novaya Zemlya.

3.2. TWO RELEASE SCENARIOS

The White Book gives information on the location and time of disposal of the various waste forms. The liquid and solid radioactive waste is here assumed to be instantly available in soluble form for dispersion at the time of discharge. For the spent nuclear fuel two release scenarios have been adopted. These are based on preliminary release rates from the dumped reactor compartment of the icebreaker Lenin estimated by the IASAP Source Term Group. Simple scaling has been used to estimate release rates from other dumped reactor compartments based on revised estimates of total activities at the time of dumping.

One scenario (1) represents a worst-case calculation and assumes release of radionuclides from the nuclear fuel to the seawater ignoring possible containment (e.g. fuel encapsulation and reactor tank). The rate of release is thus determined by the corrosion of the fuel by the seawater. This scenario gives conservatively high consequences by not considering the barriers that delay the access of fresh seawater to the fuel and subsequently the fuel corrosion. The other scenario (2) is a more probable one that does take into account various containment barriers thus allowing for further decay of the shorter-lived radionuclides prior to release to seawater. The scenario furthermore includes an assumption of a massive event occurring at about 100 years after dumping resulting in a significant increased release of radionuclides to the environment. The total amounts of radionuclides released assumed for the calculations are shown in Table 2.

Table 2. Total ⋅ ʰ gr᷄ ᴵⱼ releases of liquid and solid radioactive waste, and spent nuclear fuel (ⁱ ᴵᴵⱼ,¹ into the Kara Sea and Barents Sea assumed for the calculations of the two scenaric ᵥ.

Nuclides	LRW +ᶜ ˣ ,ʳ	SNF1	SNF2	Total Scenario1 (worst case)	Total Scenario2 (probable case)
H-3	363			363	363
Co-60	363	113	0.0001	476	363
Ni-63		179	0.2	179	0.2
Sr-90	363	2180	271	2543	634
I-129		0.001	0.002	0.001	0.002
Cs-137	363	2366	318	2729	681
Pu-239		11	10	11	10
Am-241		9	8	9	8
Total	1451	4858	607	6309	2058

The two release scenarios are shown in graphical form in Figures 4, 5 and 6. Figure 4 shows the assumed release from LRW and SRW with time to the Arctic waters. The peak in 1976 is related to a discharge of liquid reactor waste to the Kara Sea from the nuclear icebreaker Lenin and the peak in 1988 from a discharge of liquid waste in the Barents Sea. The Figures 5 and 6 show the assumed releases of radioactivity to the Arctic waters from the spent nuclear fuel. Figure 5 shows the assumptions for Scenario 1 (worst case) which is characterised by declining releases from the time of dumping for all radionuclides except for ^{241}Am which grows in from ^{241}Pu. Figure 6 shows the assumptions for Scenario 2 which gives lower release rates than for Scenario 1; the time course is characterised by the assumption of a major event about 100 years after the time of dumping which causes a marked increase in the rate of release for most radionuclides. As seen from Table 2, a total release of about 6 PBq is assumed for Scenario 1 and about 2 PBq for Scenario 2.
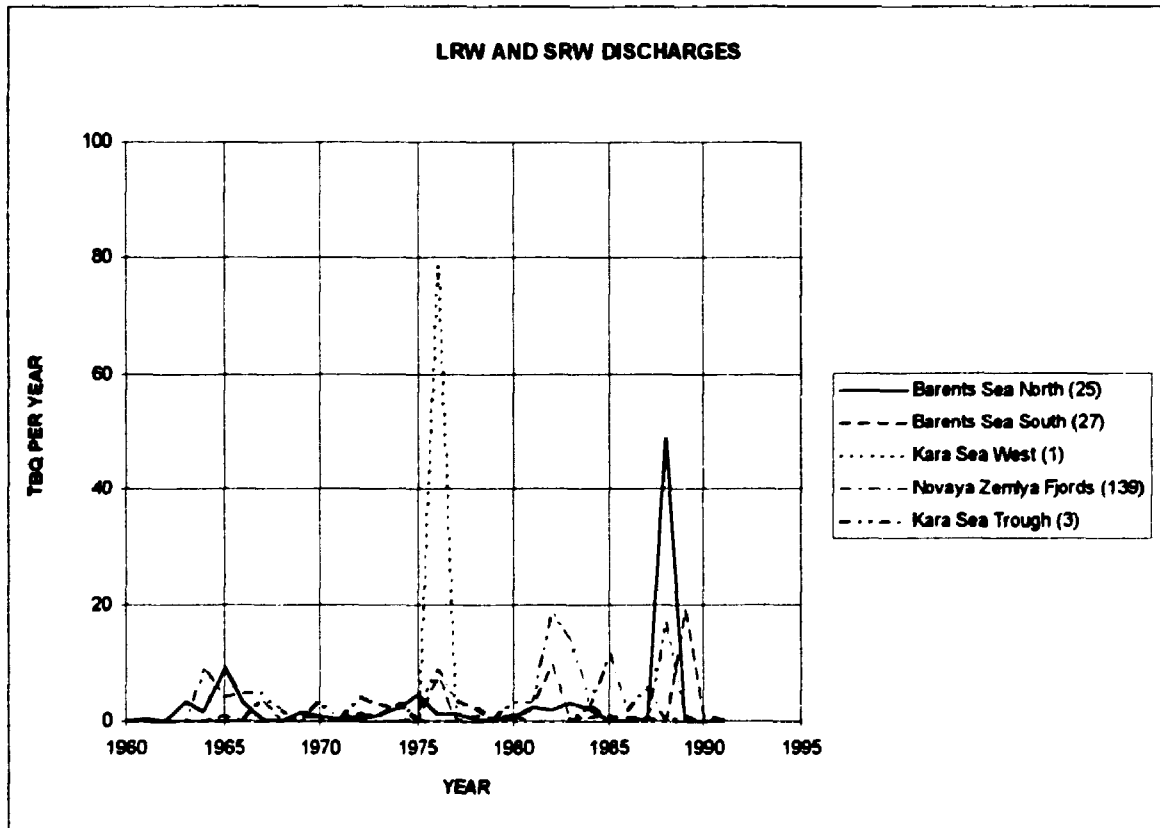
Figure 4. Release of liquid and solid radioactive waste with time (TBq y^{-1}) in Arctic waters for the radionuclides ^{3}H, ^{60}Co, ^{90}Sr and ^{137}Cs (assumed to occur in equal amounts of activity for each nuclide).
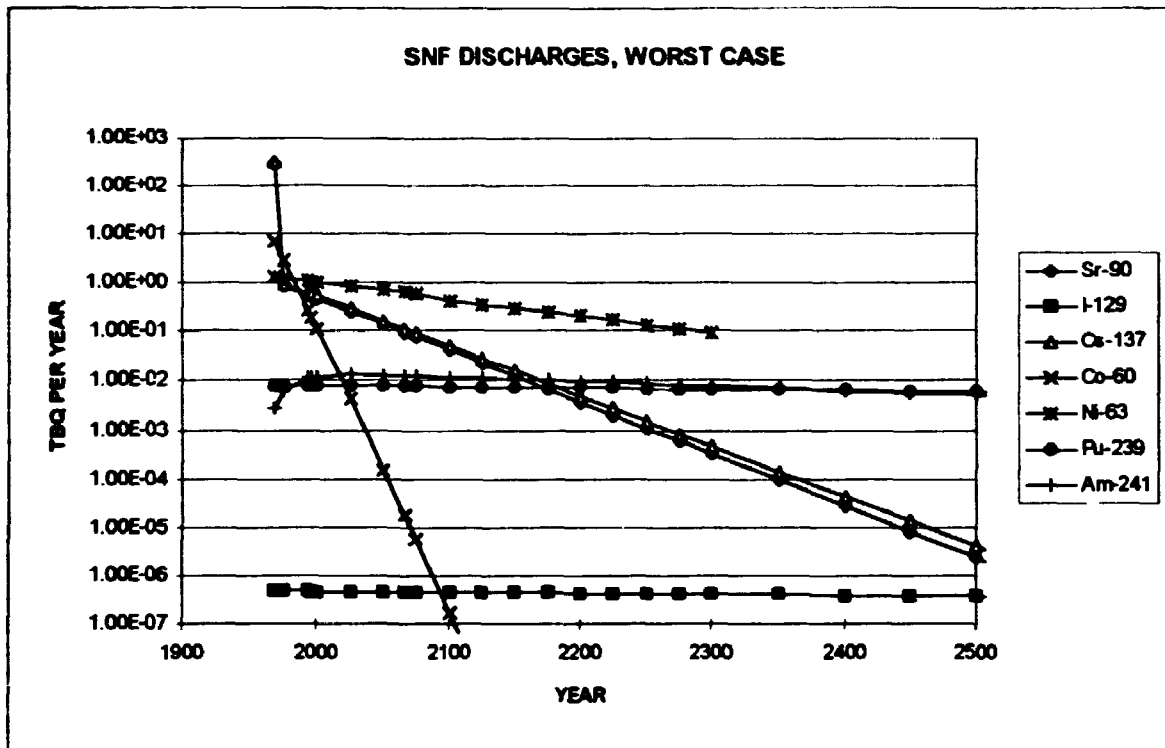
Figure 5. Assumed rate of release of radioactivity (TBq y^{-1}) from spent nuclear fuel for worst-case scenario.
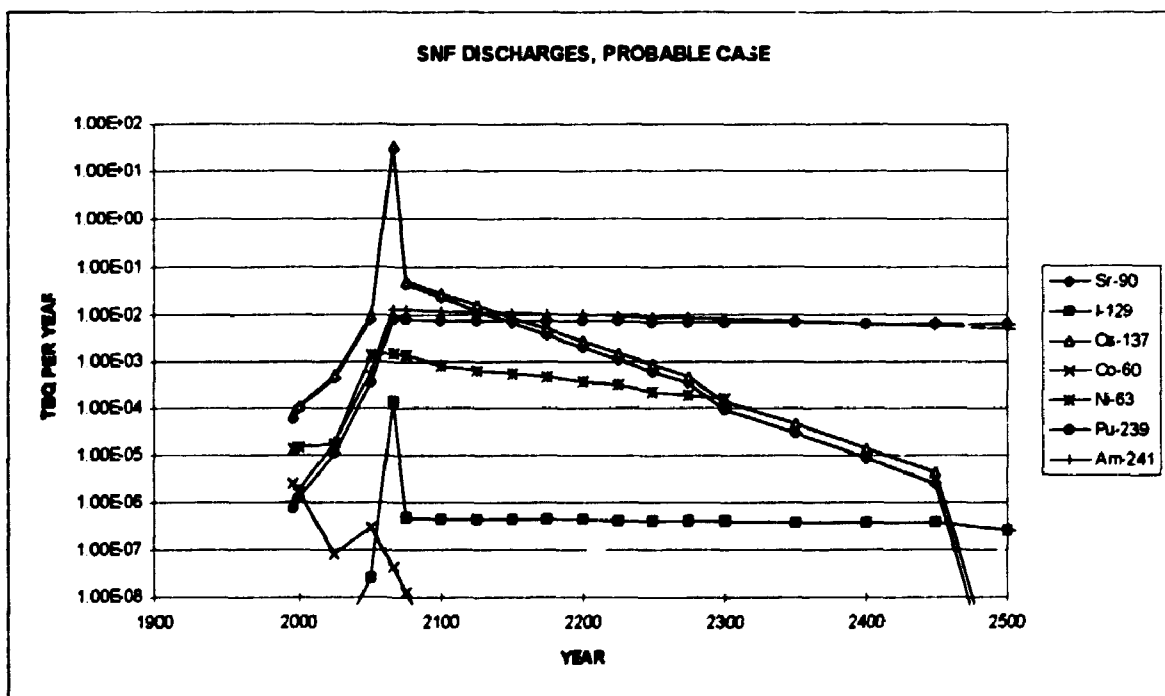

Figure 6. Assumed rate of release of radioactivity (TBq y^{-1}) from spent nuclear fuel for probable-case scenario.

4. RESULTS

4.1. DOSES FROM DISCHARGES OF UNIT ACTIVITY

The results of the calculations of the unit discharges of 1 TBq for the radionuclides ^{3}H, ^{60}Co, ^{90}Sr, ^{137}Cs, ^{239}Pu and ^{241}Am into the Kara Sea and the Barents Sea are shown in graphs for selected locations in Appendix B. These graphs give unfiltered seawater concentrations (Bq m^{-3}), surface sediment concentrations (Bq kg^{-1} dw) and collective doses (manSv) shown as a function of time. An overview of the results is given in Table 3 which lists the relative collective doses in different regions. The table also gives the absolute values of the collective doses integrated to 1000 years and indicates the dominating exposure pathways.

Table 3. Collective doses in different regions for each radionuclide from discharges of unit activity (1 TBq) into a generic fjord located on the east coast of Novaya Zemlya. The doses are given in percent of the dose from the dominating pathway. Total doses are given in mansieverts.

Region (box no.)	H-3	Co-60	Ni-63	Sr-90	I-129	Cs-137	Pu-239	Am-241
Barents Sea (25+27)	66%	60%	30%	53%	10%	54%	3%	1%
Norwegian Sea (32)	11%	16%	11%	11%	5%	11%	2%	2%
Denmark Strait (35)	4%	4%	4%	5%	2%	5%	1%	1%
Faroe Channel (38)	2%	1%	4%	3%	3%	3%	1%	1%
Labrador Sea (43)	4%	2%	8%	6%	5%	7%	15%	33%
North American Basin (45)	0.3%	0.1%	2%	1%	3%	1%	8%	11%
Sargasso Sea (51)	0.1%	0.02%	2%	1%	2%	1%	3%	4%
Cap Verde Basin (53)	1%	0.2%	8%	3%	9%	4%	6%	6%
Other Oceans (59)	0.1%	0.004%	8%	1%	40%	1%	38%	19%
Scottish Waters West (61)	1%	1%	2%	2%	2%	2%	1%	0.3%
French Continental Shelf (87)	0.1%	0.1%	0.3%	0.2%	0.2%	0.2%	4%	8%
North Sea Central (107)	1%	0.1%	1%	1%	1%	1%	0.2%	0.02%
North Sea North (111)	1%	0.4%	2%	2%	2%	2%	0.4%	0.1%
Collective dose (manSv)	3E-08	5E-05	3E-05	1E-04	4E-02	3E-03	3E-02	1E-03
Dominating pathway	Fish	Fish	Fish	Fish	Fish	Fish	Mollusc	Mollusc

For ^{3}H, ^{60}Co, ^{90}Sr and ^{137}Cs the relative geographical dose distributions are quite similar and fish consumption is the dominating exposure pathway. For the longer-lived nuclides ^{63}Ni, ^{129}I, ^{239}Pu and ^{241}Am the relative geographical dose distributions are different, giving rise to collective doses in regions far from the Arctic waters. The nuclides ^{129}I and ^{239}Pu give the highest collective dose per unit discharge, while ^{3}H gives the lowest. Ingestion of fish is the dominating exposure pathway for all the nuclides except for ^{239}Pu and ^{241}Am where the collective dose is dominated by the consumption of molluscs.

4.2. DOSES FROM TWO RELEASE SCENARIOS

The first scenario (1) represents a worst-case calculation by ignoring the isolation of the solid waste including the SNF from the seawater (e.g. the encapsulation of the nuclear fuel, the reactor vessel and the packaging). The second scenario (2) represents a more realistic case of release of activity from the solid waste taking into consideration the corrosion of the protective barriers of the dumped waste over a period of 100 y from the time of dumping. The doses have been integrated over 1000 y for ^{63}Ni, ^{90}Sr, ^{129}I, ^{137}Cs, ^{239}Pu and ^{241}Am and over 250 y for ^{3}H and ^{60}Co.

The results of the calculations are shown in Table 4 which gives the collective doses for each radionuclide and the total collective doses for the two release scenarios.

Table 4. Collective doses (manSv, rounded) calculated to 1000 years for the two release scenarios.

Nuclide	Scenario 1 worst case (manSv)	(%)	Scenario 2 probable case (manSv)	(%)
Cs-137	7.9	87	2.3	73
Co-60	0.47	5	0.46	15
Sr-90	0.39	4	0.11	3
Pu-239	0.28	3	0.26	8
Am-241	0.01	0.1	0.01	0.2
Ni-63	0.005	0.05	5E-06	0.0001
I-129	2E-05	0.0003	6E-05	0.002
H-3	2E-05	0.0002	2E-05	0.0005
Total	9.1	100	3.2	100
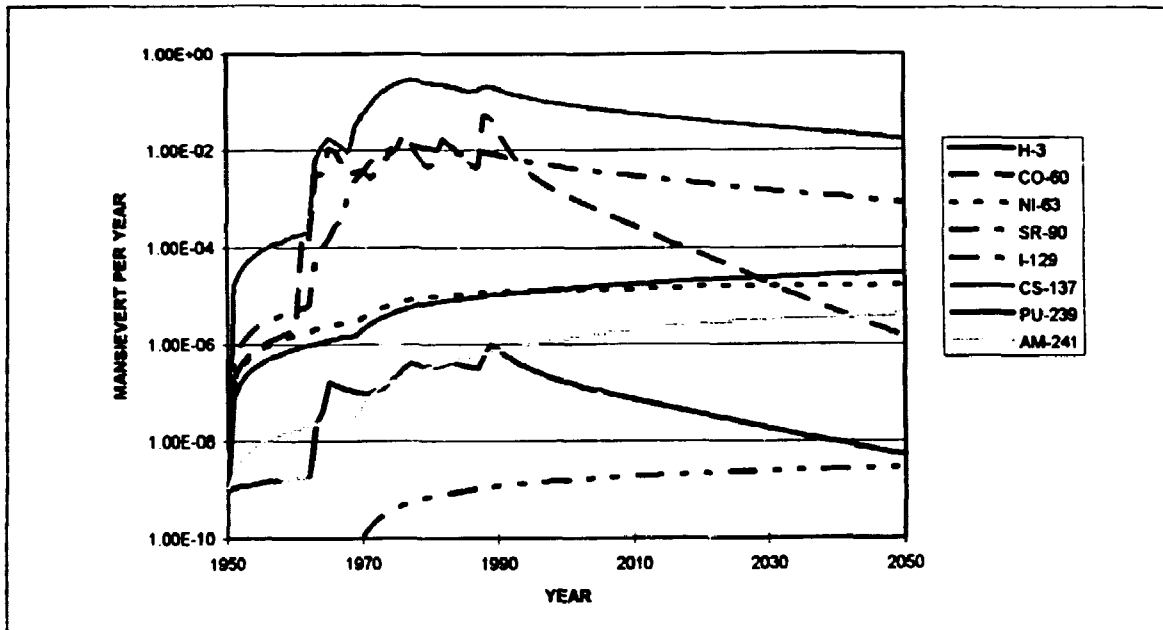
Figure 7. Collective dose rates for Scenario 1 (worst case) showing the contributions from the different radionuclides.
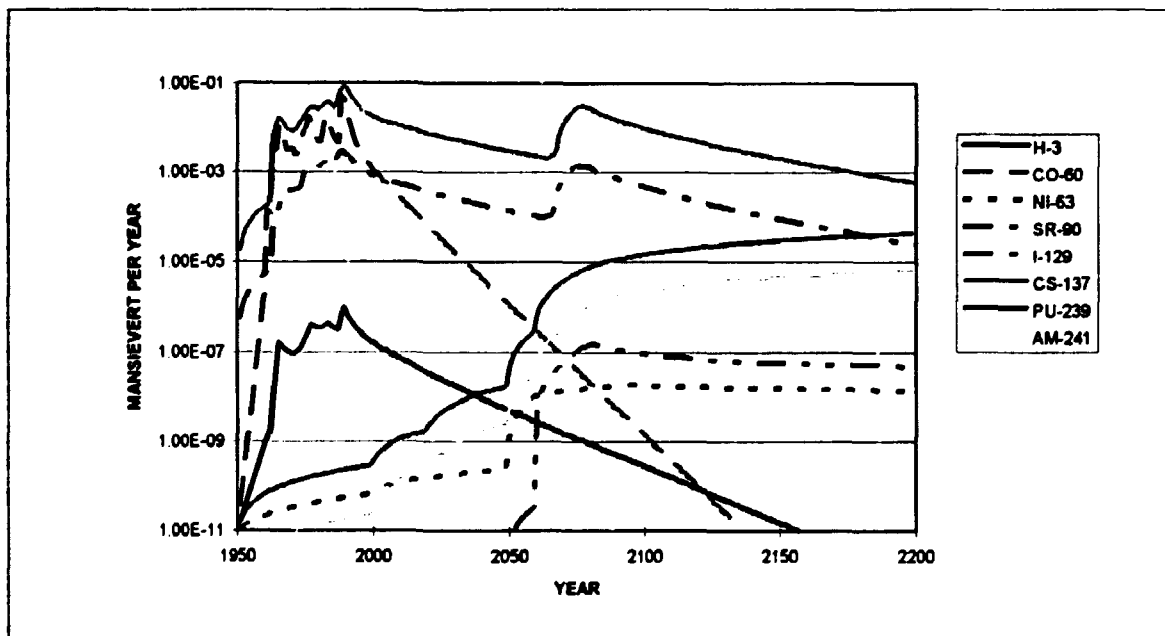
Figure 8. Collective dose rates for Scenario 2 (probable case) showing the contributions from the different radionuclides.

The total collective dose for Scenario 1 is calculated at a value of 9 manSv dominated by the contribution from ^{137}Cs (about 90%). The total collective dose for Scenario 2 is calculated at a value of 3 manSv also dominated by the contribution from ^{137}Cs (about 70%).

The collective dose rates for the two scenarios are shown in Figure 7 and Figure 8. For Scenario 1 the total collective dose rate peaks at about 0.3 manSv per year and at about 0.1 manSv per year for Scenario 2. For both scenarios ^{137}Cs and ^{60}Co are seen to

dominate the peak collective dose rate while the long-lived transuranics ^{239}Pu and ^{241}Am dominate the collective dose rates at longer time scales.

Time courses of radionuclide concentrations in seawater and surface sediments are shown in Appendix C for the worst-case release scenario in selected regions: Western Kara Sea (box 1), Barents Sea (box 27), Chuckchi Sea (box 13), Greenland Sea (box 29) and Central North Sea (box 107).

5. CONCLUSIONS

A box model for the dispersion of radionuclides in the marine environment covering the Arctic Ocean and the North Atlantic Ocean has been constructed. The model is based on updated information on water mixing in the European coastal waters, and the hydrodynamical data used in the model for the Arctic Ocean and North Atlantic Ocean are derived from a 3-dimensional World Ocean circulation model. A limited comparison of the model predictions of conservative radionuclide seawater concentrations with annual averages of measured data in European coastal waters indicates agreement within 10%. The model includes the transfer of radionuclides to seabed sediments.

The basic input data for the model have been assumed identical to those that were used in the CEC Marina study (CEC 1990). This study dealt with an assessment of the radiological exposure of the population of the European Community from radioactivity in North European marine waters. Generic values from these data were used where no other information was available. This applies especially for the Arctic waters for which limited site-specific information on concentrations of particulate matter in the water and sedimentation rates were available for this work. These two parameters are important for the prediction of dispersion in the marine environment especially with respect to the sediment-reactive radionuclides (^{60}Co, ^{63}Ni, ^{239}Pu and ^{241}Am).

Collective doses to the world population have been calculated from ingestion of radionuclides in contaminated seafood (fish, crustaceans and molluscs). The levels of contamination in seafood have been estimated from the levels in filtered seawater predicted by the model, and data on the human intake of seafood are based on fishery statistics. The ingestion pathways covered here are believed to account for the main part of the collective dose. In the Marina study these pathways accounted for 89% of the total collective dose to the European population.

The reliability of the predictions produced by the present model has not been tested quantitatively. However, it has been verified that the results (total collective doses) from the present model are not in disagreement with those from the Marina study. It is furthermore believed that the collective doses estimated in this preliminary assessment are within an order of magnitude of those obtained from using more site-specific information and based on the same radionuclide release scenarios.

Collective doses have been calculated from single releases of 1 TBq of the radionuclides ^{3}H, ^{60}Co, ^{63}Ni, ^{90}Sr, ^{129}I, ^{137}Cs, ^{239}Pu and ^{241}Am into a fjord on the east coast of Novaya Zemlya. These results show that doses for the shorter-lived radionuclides ^{3}H, ^{60}Co, ^{90}Sr and ^{137}Cs are derived mainly from seafood production in the Barents Sea. The doses from the longer-lived radionuclides ^{63}Ni and ^{129}I derive to a smaller extent from seafood production in the Barents Sea and more on seafood production from regions further from the Arctic Seas. Doses for the radionuclides ^{239}Pu and ^{241}Am are delivered through marine produce far from the Arctic Ocean.

Collective doses have furthermore been calculated for two release scenarios, both based on information of the dumping of radioactive waste in the Barents Sea and Kara Sea by the former Soviet Union (White Book No. 3, 1993) and on preliminary information from the International Arctic Sea Assessment Programme organised by the International Atomic Energy Agency. A worst-case scenario (1) has been selected according to which it was assumed that all radionuclides in liquid and solid radioactive waste were available for dispersion in the marine environment at the time of dumping, thus leaving no time for decay of short-lived radionuclides prior to release. Release of radionuclides from spent nuclear fuel (from dumped damaged nuclear reactors) was assumed by direct corrosion of the fuel ignoring the barriers that prevent direct contact between the fuel and the seawater. Another scenario (2) was selected according to which the releases of radionuclides from spent nuclear fuel were not assumed to occur until after degradation of the protective barriers. All other liquid and solid radioactive waste was assumed to be available for dispersion at the time of discharge in both scenarios.

Collective doses (calculated to 1000 years) give for the worst-case scenario a value of about 9 manSv and a value for the second scenario a value of about 3 manSv. In both cases ^{137}Cs is the radionuclide predicted to dominate the collective doses as well as the peak collective dose rates, which are about 0.3 manSv per year for Scenario 1 and about 0.1 manSv per year for Scenario 2.

A comparison with the results from the Marina study shows that the radiological sensitivity (collective dose per unit discharge, e.g. manSv per PBq) of discharges of ^{137}Cs to the Kara Sea is more than one order of magnitude lower (3 manSv PBq^{-1}) than that of discharges of ^{137}Cs to the Irish Sea (50 manSv PBq^{-1}). The main reason for this difference is the low productivity of seafood for human consumption in the Polar waters compared with that in the European coastal waters.

6. ACKNOWLEDGEMENT

7. REFERENCES

Breton, M. and Salomon, J.C., 1995. A 2D long-term advection-dispersion model for the Channel and Southern North Sea. Part A: Validation through comparison with artificial radionuclides. Accepted by Journal of Marine Systems.

Camplin, W. C., Clark, M. J. and Delow, C. E., 1982. The radiation exposure of the UK population from liquid effluents discharged from civil nuclear installations in the UK in 1978. National Radiological Protection Board, Chilton, UK.

CEC, 1990. The radiological exposure of the population of the European community from radioactivity in North European marine waters, Project 'Marina', Commission of the European Communities, Bruxelles, EUR 12483.

Chartier, M. 1993. Radiological assessment of dumping in the Kara and Barents Seas: Design of a compartmental structure for the Arctic Ocean and surrounding oceans. CETIIS, Ivry sur Seine, France.

Dozhdikov, S.I., Zhuravkov, A.M. and Zolotkov, A.A. 1993(?). Corrosion resistance of spent nuclear fuel in sea water (Translated from Russian). I.V. Kurchatov Institute of Atomic Energy, Moscow; Murmansk Marine Shipping Company.

EC, 1995. Methodology for assessing the radiological consequences of routine releases of radionuclides to the environment, European Commission, Luxembourg, EUR 15760 EN.

Hallstadius, L., Garcia-Montaño, E., Nilsson, U. and Boelskifte, S., 1987. An improved and validated dispersion model for the North Sea and adjacent waters. J. Environ. Radioactivity, 5:261-274.

IAEA, 1994. Sources of radioactivity in the marine environment and their relative contributions to overall dose assessment from marine radioactivity (MARDOS), Final Report of the CRP. IAEA-MEL-R2/94. International Atomic Energy Agency, Marine Environment Laboratory, Monaco.

Kirchner, T.B., 1989. TIME-ZERO, The integrated modeling environment, Ecological Modelling, 47:33-52.

Marti, O. 1992. Etude de l'Ocean Mondial: Modélisation de la circulation et du transport des traceurs anthropiques. Doctor thesis from University Pierre and Madame Curie, Paris.

Mount, M.E., Sheaffer, M.K. and Abbott, D.T. 1993. Estimated inventory of radionuclides in former Soviet Union naval reactors dumped in the Kara Sea. Proc. of the International Conference on Environmental Radioactivity in the Arctic and Antarctic, Kirkenes, Norway, 23-27 August 1993.

Nielsen, S.P. and Aarkrog, A., 1988. A model performance test for the aquatic dispersion of radionuclides in the North-East Atlantic waters. In: Proceedings of the workshop on "Methods for Assessing the Reliability of Environmental Transfer Model Predictions" held in Athens, 5-9 October 1987. Commission of the European Communities, Bruxelles, EUR 11367.

Nielsen, S.P., 1995. A box model for North-East Atlantic coastal waters compared with radioactive tracers. Accepted by Journal of Marine Systems.

NRPB and CEA, 1979. Methodology for evaluating the radiological consequences of radioactive effluents released in normal operations, Commission of the European Communities, Bruxelles, Doc. No. V/3865/1/,9-EN.

Platovskikh, Y.A., Rubanov, S.M. and Sergeev, I.V. 1992. Ecological problems caused by the sinking of a nuclear vessel (Translated from Russian). A.N. Krylov Central Scientific Research Institute.

Schönfeld, W., 1995. Numerical simulation of the dispersion of artificial radionuclides in the English Channel and the North Sea. Accepted by Journal of Marine Systems.

Sivintsev, Y. 1993. The sedbed sources of radionuclides in the dumped reactor compartment of atomic icebreaker "Lenin". Proc. of the International Conference on Environmental Radioactivity in the Arctic and Antarctic, Kirkenes, Norway, 23-27 August 1993.

White Book No. 3, 1993. Facts and Problems Related to Radioactive Waste Disposal in Seas Adjacent to the Territory of the Russian Federation. Materials for a Report by the Government Commission on Matters Related to Radioactive Waste Disposal at Sea, Created by Decree No. 613 of the Russian Federation President, October 24, 1992; Moscow.

Ådlandsvik, B. 1993. Norwegian Institute of Marine Research, Bergen. Personal communication.

8. APPENDIX A, Basic model input data

This appendix contains tables that list the numerical input information on which the box model is based.

Table A1. List of model water boxes giving box numbers, names of regions, volumes (m³), mean depths (m), suspended sediment loads (SSL, t m⁻³) and sedimentation rates (SR, t m⁻² y⁻¹).

Box No.	Region	Volume (m³)	Depth (m)	SSL (t m⁻³)	SR (t m⁻² y⁻¹)
1	Western Kara Sea	1.2E+13	7.0E+01	3E-06	1E-03
3	Western Kara Sea deep	1.6E+13	2.5E+02	6E-06	3E-04
5	Eastern Kara Sea	7.0E+13	7.0E+01	3E-06	1E-03
7	Laptev Sea, upper	2.2E+14	3.3E+02	3E-06	1E-04
8	Laptev Sea, lower	4.8E+14	7.0E+02	1E-06	2E-05
10	Eurasin Basin, upper	2.7E+14	3.3E+02	1E-06	1E-04
11	Eurasin Basin, lower	2.7E+15	3.2E+03	1E-06	2E-05
13	East Siberian Sea, upper	3.6E+14	3.3E+02	1E-06	1E-04
14	East Siberian Sea, lower	9.9E+14	9.0E+02	1E-06	2E-05
16	Beaufort Sea, upper	2.6E+14	3.3E+02	1E-06	1E-04
17	Beaufort Sea, lower	8.8E+14	1.2E+03	1E-06	2E-05
19	Canadian Arctic Sea, upper	2.1E+14	3.3E+02	1E-06	1E-04
20	Canadian Arctic Sea, lower	1.4E+15	2.2E+03	1E-06	2E-05
22	Makarov and Fram Basins, upper	4.7E+14	3.3E+02	1E-06	1E-04
23	Makarov and Fram Basins, lower	4.1E+15	2.9E+03	1E-06	2E-05
25	Barents Sea North	1.6E+14	2.0E+02	6E-06	5E-04
27	Barents Sea South	1.6E+14	2.0E+02	6E-06	1E-03
29	Greenland Sea, upper	2.5E+14	3.3E+02	1E-06	1E-04
30	Greenland Sea, lower	1.4E+15	1.8E+03	1E-06	2E-05
32	Norwegian Sea, upper	2.9E+14	3.3E+02	1E-06	1E-04
33	Norwegian Sea, lower	1.7E+15	1.9E+03	1E-06	2E-05
35	Denmark Strait, upper	1.3E+14	3.3E+02	1E-06	1E-04
36	Denmark Strait, lower	8.0E+13	2.0E+02	1E-06	2E-05
38	Faroe Channel	1.9E+15	1.4E+03	1E-06	1E-04
40	Irminger Basin, upper	1.3E+14	3.3E+02	1E-06	1E-04
41	Irminger Basin, lower	1.1E+15	2.7E+03	1E-06	2E-05
43	Labrador Sea	6.0E+15	2.0E+03	1E-06	2E-05
45	North American Basin	1.9E+16	4.5E+03	1E-06	2E-05
47	Central North Atlantic	1.5E+16	4.0E+03	1E-06	2E-05
49	Western Europe Basin	2.2E+15	2.7E+03	1E-06	2E-05
51	Sargasso Sea	4.6E+16	3.5E+03	1E-06	2E-05
53	Cap Verde Basin	4.0E+16	4.5E+03	1E-06	2E-05
55	Guyana Basin	1.3E+16	4.0E+03	1E-06	2E-05
57	Gulf of Guinea	5.6E+15	4.7E+03	1E-06	2E-05
59	Remaining World Ocean	1.1E+18	3.8E+03	1E-06	2E-05
61	Scottish Waters West	1.0E+13	1.1E+02	1E-06	1E-04
63	Scottish Waters East	3.0E+12	1.1E+02	1E-06	1E-04

Table A1. Continued

Box No.	Region	Volume (m³)	Depth (m)	SSL (t m⁻³)	SR (t m⁻² y⁻¹)
65	Irish Sea North West	4.1E+11	9.3E+01	3E-06	2E-03
67	Irish Sea North	6.0E+10	3.4E+01	3E-06	5E-03
69	Irish Sea North East	5.2E+10	2.4E+01	3E-06	5E-03
71	Irish Sea West	6.6E+11	6.3E+01	3E-06	2E-03
73	Irish Sea South East	1.6E+11	3.1E+01	3E-06	5E-03
75	Cumbrian Waters	3.8E+10	2.8E+01	3E-06	5E-03
77	Irish Sea South	1.1E+12	5.7E+01	1E-06	1E-04
79	Liverpool and Morcambre Bay	3.2E+10	1.3E+01	3E-06	5E-03
81	Celtic Sea	2.0E+13	1.5E+02	1E-06	1E-04
83	Bristol Channel	1.0E+12	5.0E+01	1E-06	1E-04
85	Bay of Biscay	6.5E+14	4.0E+03	1E-06	1E-05
87	French Continental Shelf	3.5E+13	3.5E+02	1E-06	1E-04
89	Cantabrian Sea	3.0E+13	7.6E+02	1E-06	2E-04
91	Portuguese Continental Shelf	1.5E+13	4.9E+02	1E-06	2E-04
93	Gulf of Cadiz	2.3E+14	1.7E+03	1E-06	5E-05
95	Mediterranean Sea	4.0E+15	1.3E+03	1E-06	1E-04
97	English Channel West	3.2E+12	6.0E+01	1E-06	1E-04
99	English channel South East	6.5E+11	4.0E+01	1E-06	1E-04
101	English Channel North East	6.5E+11	4.0E+01	1E-06	1E-04
103	North Sea South West	4.5E+11	3.1E+01	6E-06	1E-04
105	North Sea South East	9.5E+11	3.7E+01	6E-06	1E-04
107	North Sea Central	1.3E+13	5.0E+01	6E-06	1E-04
109	North Sea East	1.2E+12	2.2E+01	6E-06	1E-04
111	North Sea North	5.6E+13	2.4E+02	6E-06	1E-04
113	Skagerrak	6.8E+12	2.1E+02	1E-06	5E-04
115	Kattegat, deep	2.0E+11	1.0E+02	1E-06	5E-04
117	Kattegat, surface	3.2E+11	2.0E+01	1E-06	5E-04
119	Belt Sea, deep	1.4E+11	3.0E+01	1E-06	5E-04
121	Belt Sea, surface	1.5E+11	1.4E+01	1E-06	5E-04
123	Baltic Sea West, deep	7.7E+11	1.1E+02	1E-06	5E-04
125	Baltic Sea East, deep	1.5E+12	1.1E+02	1E-06	5E-04
127	Baltic Sea West, surface	3.8E+12	4.9E+01	1E-06	5E-04
129	Baltic Sea East, surface	7.0E+12	5.3E+01	1E-06	5E-04
131	Bothnian Sea	4.9E+12	6.2E+01	1E-06	5E-04
133	Bothnian Bay	1.5E+12	4.1E+01	1E-06	5E-04
135	Gulf of Finland	1.1E+12	3.7E+01	1E-06	5E-04
137	Gulf of Riga	4.1E+11	2.3E+01	1E-06	5E-04

Table A2. Exchange rates of water between adjacent boxes ($km^3 y^{-1}$).

From box	To box	Flux ($km^3 y^{-1}$)	From box	To box	Flux ($km^3 y^{-1}$)	From box	To box	Flux ($km^3 y^{-1}$)
1	3	3.2E+03	38	33	1.5E+05	81	85	1.5E+05
1	5	9.5E+02	38	35	2.3E+04	81	87	1.4E+05
1	27	9.5E+02	38	36	1.8E+05	81	97	7.0E+03
3	1	3.2E+03	38	40	2.1E+05	83	81	2.0E+03
5	1	9.5E+02	38	49	2.6E+05	85	49	6.7E+05
5	7	8.5E+03	38	61	8.3E+03	85	81	1.5E+05
5	22	5.2E+04	38	111	3.4E+04	85	87	5.8E+05
5	25	9.5E+03	40	35	1.7E+05	85	89	3.9E+05
7	8	3.7E+04	40	38	1.4E+05	87	81	1.4E+05
7	10	6.9E+04	40	41	6.3E+04	87	85	5.8E+05
7	22	1.8E+04	40	43	3.3E+05	87	89	7.5E+04
8	7	2.1E+04	40	49	9.6E+04	89	49	1.1E+05
8	11	1.3E+05	41	40	1.3E+04	89	85	3.9E+05
10	7	2.9E+04	41	43	8.0E+05	89	87	7.5E+04
10	11	3.3E+04	41	49	6.3E+05	89	91	1.5E+05
10	13	2.8E+03	43	40	2.1E+05	91	53	4.6E+05
10	19	1.6E+05	43	41	4.7E+05	91	89	1.5E+05
10	22	1.0E+05	43	47	1.1E+06	91	93	6.0E+04
11	8	5.5E+04	45	47	6.8E+05	93	53	5.1E+05
11	10	2.2E+04	45	51	1.5E+06	93	91	5.8E+04
11	20	8.8E+04	47	43	6.2E+05	93	95	5.3E+04
11	23	1.1E+05	47	45	3.1E+05	95	93	5.1E+04
13	10	1.9E+05	47	49	9.9E+05	97	81	2.0E+03
13	14	1.4E+05	47	53	5.3E+05	97	99	3.5E+03
14	11	4.6E+04	49	38	7.6E+05	97	101	3.5E+03
14	13	1.4E+05	49	40	2.1E+05	99	97	1.0E+03
16	13	1.5E+05	49	41	4.5E+05	99	101	3.0E+02
16	17	4.5E+04	49	47	5.5E+05	99	105	6.0E+03
16	19	4.7E+03	49	81	1.2E+04	101	97	1.0E+03
17	14	4.7E+04	49	85	6.7E+05	101	99	3.7E+03
17	16	5.6E+04	49	89	1.1E+05	101	105	5.0E+01
17	20	1.5E+04	51	45	1.9E+06	103	105	6.1E+02
19	16	1.5E+05	51	53	6.7E+05	103	107	3.8E+02
19	20	3.2E+04	51	55	1.1E+06	105	99	5.0E+01
19	22	1.8E+04	53	47	1.2E+05	105	101	1.0E+03
19	43	1.4E+04	53	51	1.2E+06	105	103	2.9E+02
20	17	7.4E+04	53	57	1.6E+05	105	107	4.6E+02
20	19	2.2E+04	53	91	4.6E+05	105	109	7.3E+03
20	23	8.0E+04	53	93	5.1E+05	107	63	0.0E+00
22	7	6.5E+04	55	51	8.7E+05	107	103	7.0E+02
22	10	4.7E+04	55	57	4.9E+05	107	105	0.0E+00
22	19	2.5E+04	55	59	1.1E+06	107	109	9.7E+03
22	23	3.2E+04	57	53	3.4E+05	107	111	6.9E+03

From box	To box	Flux (km³ y⁻¹)	From box	To box	Flux (km³ y⁻¹)	From box	To box	Flux (km³ y⁻¹)
22	25	1.6E+04	57	55	1.4E+05	107	113	5.6E+03
22	29	9.1E+04	57	59	6.1E+05	109	105	2.4E+03
22	43	1.4E+04	59	13	2.8E+04	109	107	8.7E+03
23	8	6.0E+04	59	55	1.2E+06	109	113	5.9E+03
23	11	6.9E+04	59	57	4.4E+05	111	38	5.0E+04
23	20	4.0E+04	61	38	5.0E+02	111	63	0.0E+00
23	22	4.6E+04	61	63	1.1E+04	111	107	0.0E+00
23	30	1.2E+04	61	65	5.0E+03	111	113	5.0E+03
25	5	6.9E+04	63	61	5.0E+02	113	107	5.5E+03
25	22	8.5E+03	63	107	8.0E+03	113	109	0.0E+00
25	27	9.5E+03	63	111	2.4E+03	113	111	1.2E+04
25	32	1.9E+04	65	61	7.4E+03	113	115	1.5E+03
27	1	9.5E+02	65	67	3.3E+02	115	117	9.3E+02
27	25	7.7E+04	65	71	5.1E+02	115	119	7.2E+02
27	32	3.2E+04	67	65	8.3E+02	117	113	2.0E+03
29	22	4.7E+04	67	69	1.8E+02	117	115	1.0E+02
29	30	9.2E+04	67	73	1.7E+02	119	121	9.3E+02
29	32	2.0E+04	69	67	2.9E+02	119	125	2.2E+02
29	35	1.9E+05	69	75	1.0E+02	119	129	2.7E+02
30	23	2.2E+03	71	65	2.4E+03	121	117	1.2E+03
30	29	3.0E+04	71	73	9.3E+02	121	119	7.0E+02
30	33	6.1E+04	71	77	6.0E+02	123	121	2.2E+02
30	36	1.4E+05	73	67	5.7E+02	123	125	2.2E+02
32	25	4.4E+03	73	71	4.3E+02	123	127	2.0E+02
32	27	9.9E+04	73	75	2.3E+02	125	123	4.4E+02
32	29	2.3E+05	73	77	7.5E+01	125	129	2.1E+02
32	33	7.4E+04	73	79	1.3E+02	127	121	7.2E+02
32	38	6.3E+03	75	69	2.0E+02	127	123	2.0E+02
33	30	1.3E+05	75	73	1.5E+02	127	129	4.4E+03
33	32	4.6E+04	75	79	3.5E+01	129	125	2.1E+02
33	38	1.1E+05	77	71	3.0E+03	129	127	4.1E+03
35	36	1.9E+05	77	73	7.5E+01	129	131	7.7E+02
35	38	7.4E+04	77	81	6.0E+02	129	135	8.0E+00
35	40	1.6E+05	79	73	1.1E+02	129	137	3.1E+02
36	35	2.8E+04	79	75	5.5E+01	131	127	9.7E+02
36	38	2.8E+04	81	49	4.6E+03	131	133	3.7E+02
36	41	4.5E+05	81	77	3.0E+03	133	131	4.7E+02
38	32	3.0E+05	81	83	2.0E+03	135	129	1.3E+02

Table A3. Nuclide-specific data used in the calculations: Halflives, sediment concentration factors (K_d), biological concentration factors (CF) for fish, crustaceans and molluscs, and factors (DF) for dose per unit intake by ingestion.

Nuclide	Halflife (y)	Kd ($m^3 t^{-1}$)	CF (fish)	CF (crustacea)	CF (mollusc)	DF ($Sv\ Bq^{-1}$)
H-3	12.3	1	1	1	1	1.8E-11
Co-60	5.27	200000	1000	5000	5000	3.4E-09
Sr-90	29.1	1000	2	2	1	2.8E-08
Cs-137	30.0	3000	100	30	30	1.3E-08
Pu-239	24100	10u000	40	300	3000	2.5E-07
Am-241	433	2000000	50	500	20000	2.0E-07
Ni-63	96	100000	1000	1000	2000	1.5E-10
I-129	15700000	20	10	10	10	1.1E-07

Table A4. Quantities of marine produce $(t\ y^{-1})$ of fish, crustacea and molluscs used in the calculations.

Box No.	Region	Fish ($t\ y^{-1}$)	Crustacea ($t\ y^{-1}$)	Molluscs ($t\ y^{-1}$)
25	Barents Sea North	3.6E+05	1.7E+04	4.4E+02
27	Barents Sea South	3.6E+05	1.7E+04	4.4E+02
29	Greenland Sea, upper	5.0E+02	8.8E+01	
32	Norwegian Sea, upper	7.3E+05	6.0E+03	5.5E+03
35	Denmark Strait, upper	3.1E+05	5.3E+03	4.0E+03
38	Faroe Channel	5.5E+05	5.4E+03	5.1E+03
40	Irminger Basin, upper	2.7E+04	3.8E+03	1.0E+00
43	Labrador Sea	1.1E+06	1.3E+05	3.7E+05
45	North American Basin	1.1E+06	1.3E+05	3.7E+05
47	Central North Atlantic	9.1E+04		
49	Western Europe Basin	1.3E+05	9.1E+02	1.4E+03
51	Sargasso Sea	1.0E+06	2.1E+05	1.7E+05
53	Cap Verde Basin	3.2E+06	5.6E+04	1.8E+05
55	Guyana Basin	2.0E+05	4.0E+04	4.0E+04
57	Gulf of Guinea	6.0E+05	1.0E+04	3.0E+04
59	Remaining World Ocean	5.6E+07	3.4E+06	6.0E+06
61	Scottish Waters West	3.3E+05	7.0E+03	4.8E+03
63	Scottish Waters East	1.0E+05	1.9E+03	1.3E+03
65	Irish Sea North West	7.1E+03	1.1E+03	1.7E+03
67	Irish Sea North	1.1E+03	3.7E+02	5.8E+02
69	Irish Sea North East	9.0E+02	8.4E+02	1.3E+03
71	Irish Sea West	1.2E+04	1.6E+03	2.3E+03
73	Irish Sea South East	2.8E+03	4.5E+02	6.9E+02
75	Cumbrian Waters	6.6E+02	2.9E+02	4.4E+02
77	Irish Sea South	1.9E+04	2.7E+03	3.8E+03
79	Liverpool and Morcambre Bay	5.6E+02	7.8E+02	1.2E+03

Table 4. Continued.

Box No.	Region	Fish ($t\,y^{-1}$)	Crustacea ($t\,y^{-1}$)	Molluscs ($t\,y^{-1}$)
81	Celtic Sea	9.6E+04	5.4E+03	4.2E+03
83	Bristol Channel	2.5E+04	4.2E+02	2.6E+03
87	French Continental Shelf	5.3E+04	1.7E+04	1.2E+05
89	Cantabrian Sea	3.9E+05	5.4E+03	2.6E+04
91	Portuguese Continental Shelf	2.2E+05	5.1E+03	1.7E+04
93	Gulf of Cadiz	6.4E+04	5.2E+03	1.2E+04
95	Mediterranean Sea	4.2E+05	2.5E+04	1.1E+05
97	English Channel West	1.0E+05	1.1E+04	4.2E+04
99	English channel South East	3.3E+04	1.6E+03	3.8E+04
101	English Channel North East	3.3E+04	3.8E+02	1.5E+03
103	North Sea South West	2.9E+04	8.0E+02	1.5E+04
105	North Sea South East	6.1E+04	5.9E+03	7.9E+04
107	North Sea Central	2.8E+05	5.9E+03	1.3E+03
109	North Sea East	2.6E+04	2.4E+04	4.4E+04
111	North Sea North	4.1E+05	4.5E+03	1.5E+03
113	Skagerrak	1.2E+05	1.7E+03	6.7E+02
115	Kattegat, deep			1.4E+03
117	Kattegat, surface	9.20E+03	2.4E+03	
119	Belt Sea, deep			4.9E+03
121	Belt Sea, surface	4.10E+04	6.8E+01	
127	Baltic Sea West, surface	1.40E+04	4.0E+00	
129	Baltic Sea East, surface	6.20E+04		
131	Bothnian Sea	6.20E+04	1.1E-01	
133	Bothnian Bay	1.90E+04	5.9E-02	
135	Gulf of Finland	1.40E+04		
137	Gulf of Riga	5.10E+03		

9.   APPENDIX B, Results of unit releases

This appendix contains graphical presentations of selected results of the calculations of unit releases in the generic model fjord on the east coast of Novaya Zemlya. The results of seawater concentrations (not filtered), surface sediment concentrations and integrated collective doses are shown versus time. The discharges are made at year zero and calculations are made until year 1000 for the longer lived nuclides and shorter for the others. The graphs show the calculated seawater concentrations for the Western Kara Sea (box 1), the Southern Barents Sea (box 27), the Chuckchi Sea (box 13), the Greenland Sea (box 29) and the Central North Sea (box 107). the sediment concentrations are from the corresponding sediment boxes no 2, 28, 15, 31 and 108. Furthermore, the collective dose to the world population calculated from ingestion of seafood is also shown versus time.
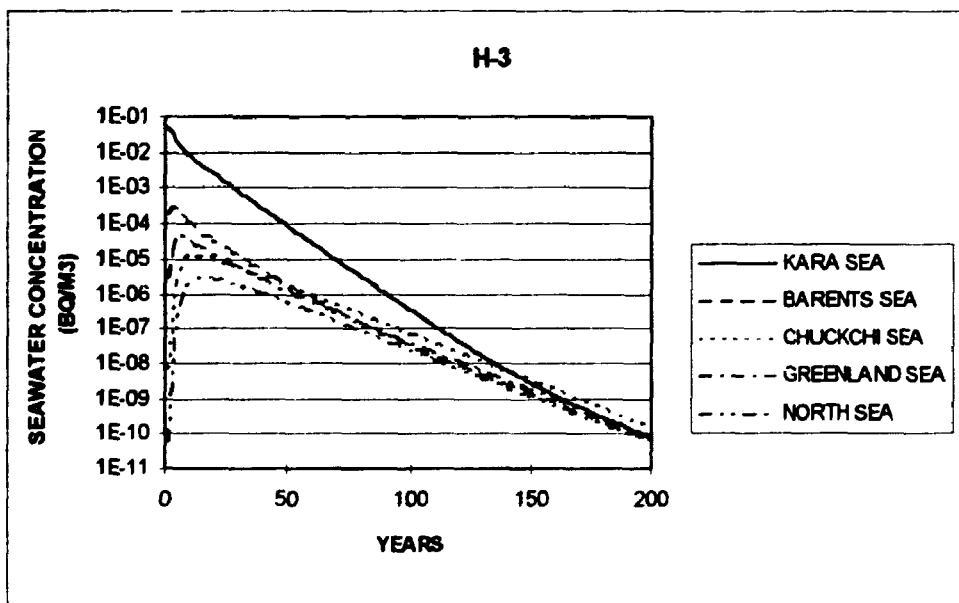
Figure B-1. Unfiltered seawater concentrations (Bq m^{-3}) in selected surface waters calculated from a single 1 TBq discharge of ^{3}H in the Novaya Zemlya fjord at year zero.
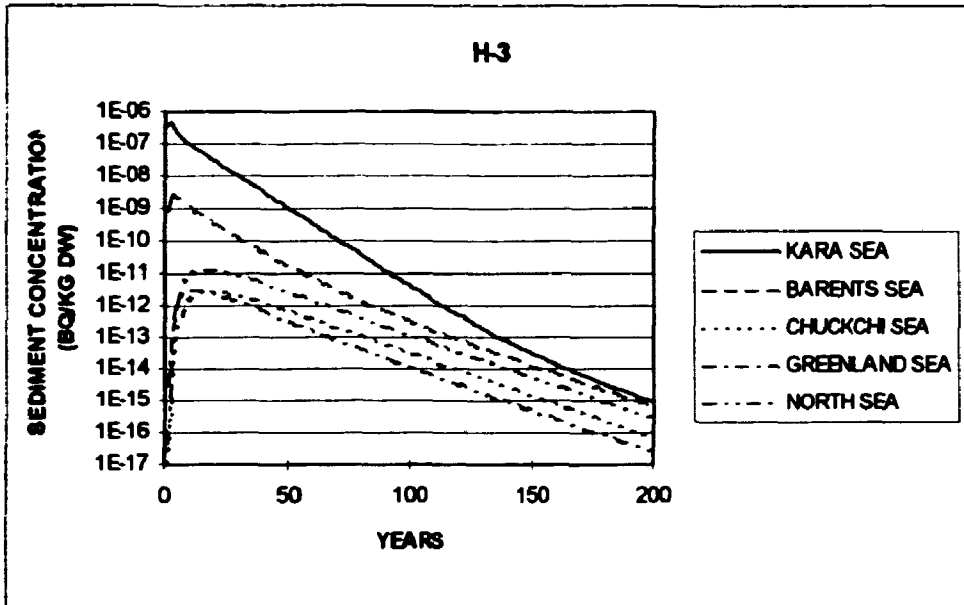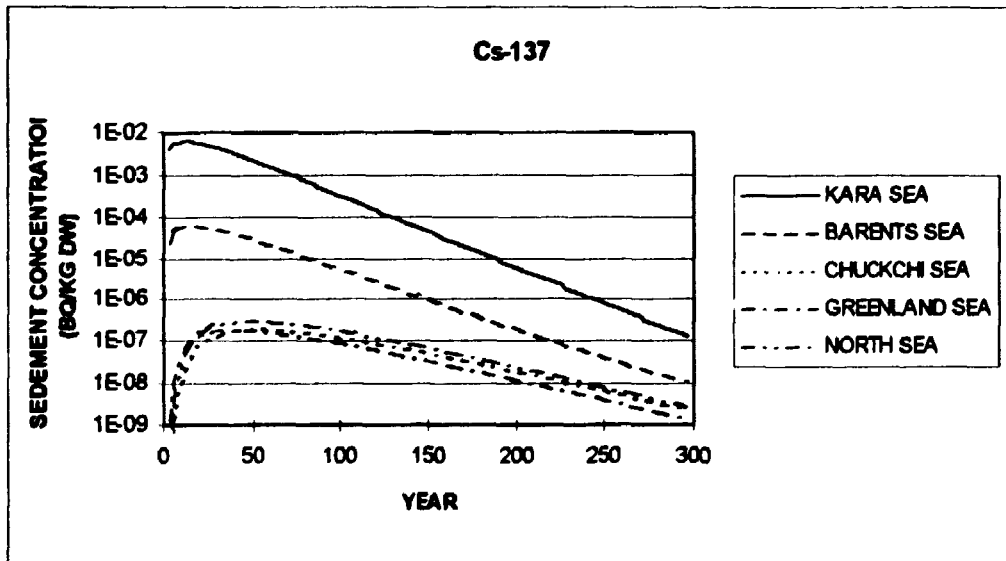
Figure B-2. Surface sediment concentrations (Bq kg^{-1} dw) in selected surface waters calculated from a single 1 TBq discharge of ^{3}H in the Novaya Zemlya fjord at year zero.
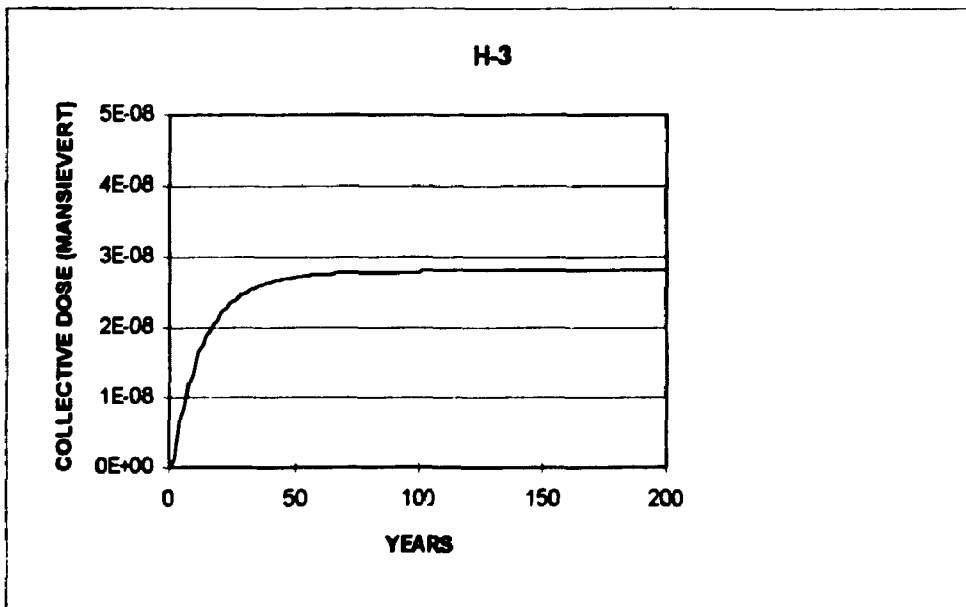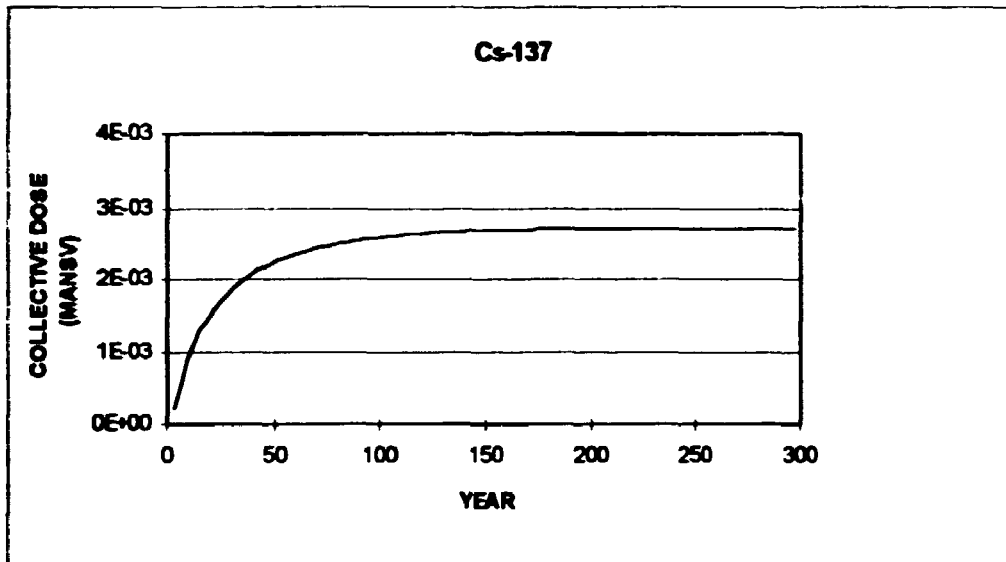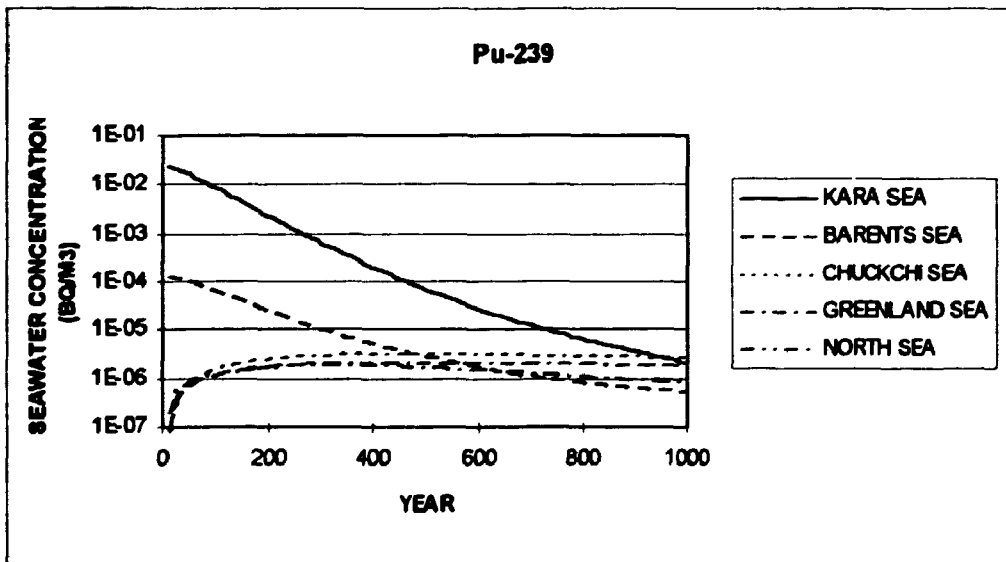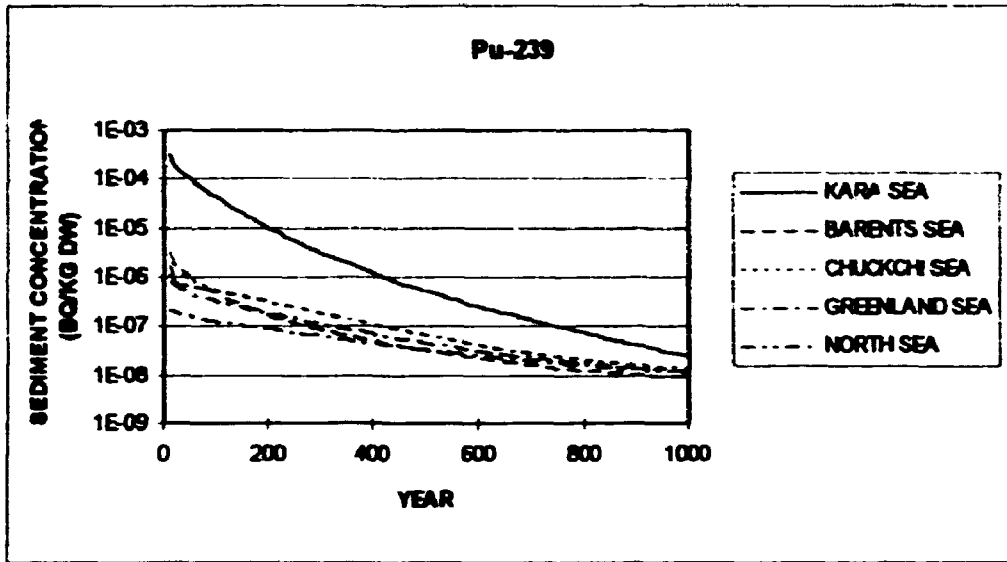

Figure B-3. Collective dose to the world population calculated from a single 1 TBq discharge of ^{3}H in the Novaya Zemlya fjord at year zero.
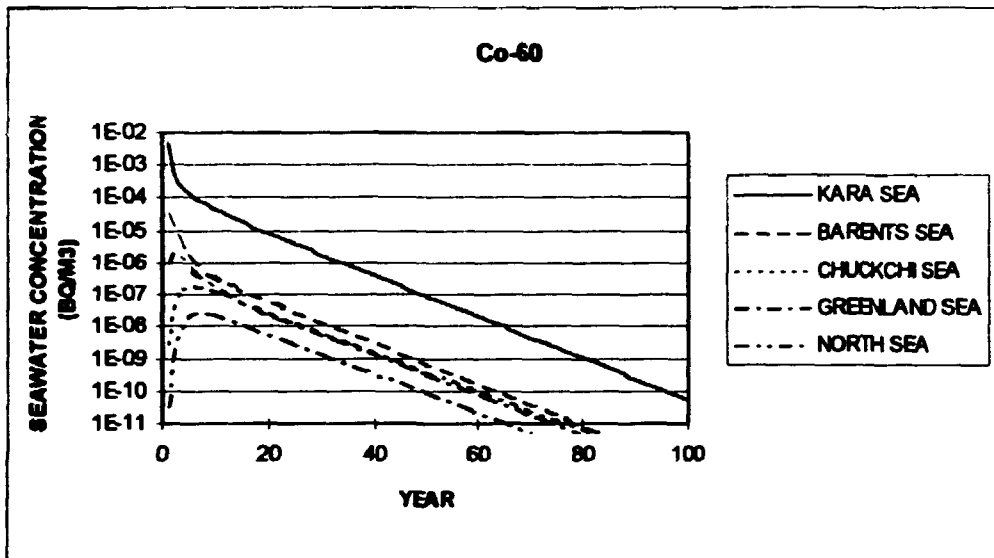
Figure B-4. Unfiltered seawater concentrations (Bq m⁻³) in selected surface waters calculated from a single 1 TBq discharge of ^{60}Co in the Novaya Zemlya fjord at year zero.
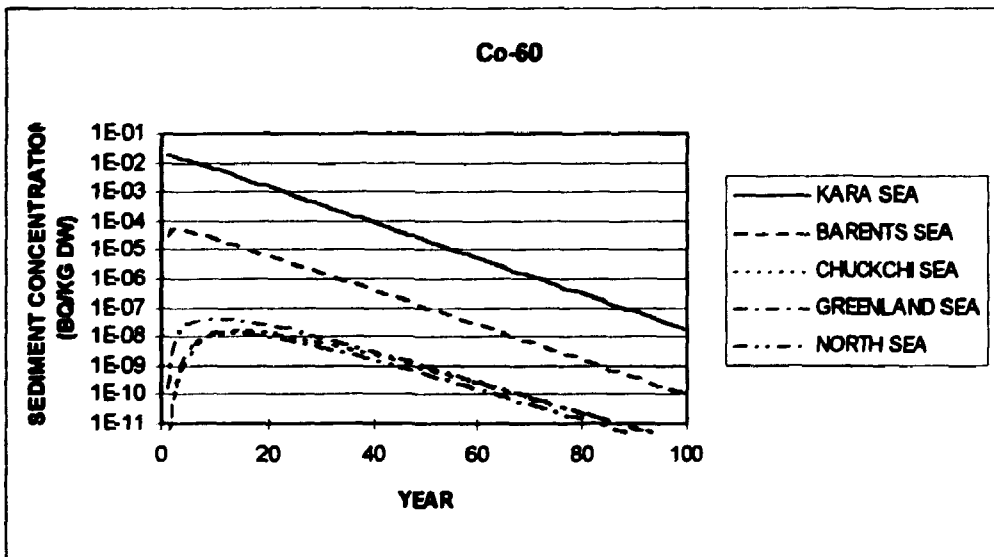
Figure B-5. Surface sediment concentrations (Bq kg⁻¹ dw) in selected surface waters calculated from a single 1 TBq discharge of ^{60}Co in the Novaya Zemlya fjord at year zero.
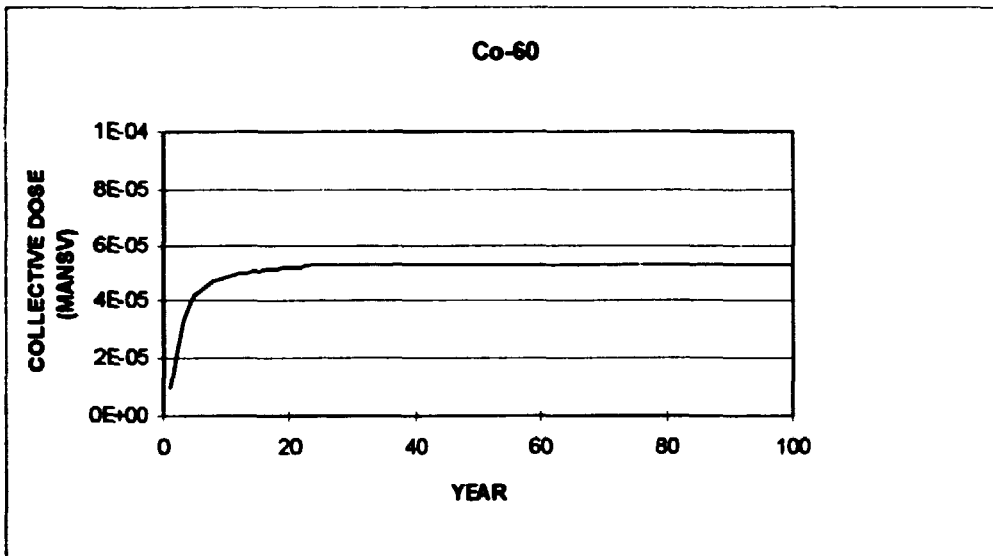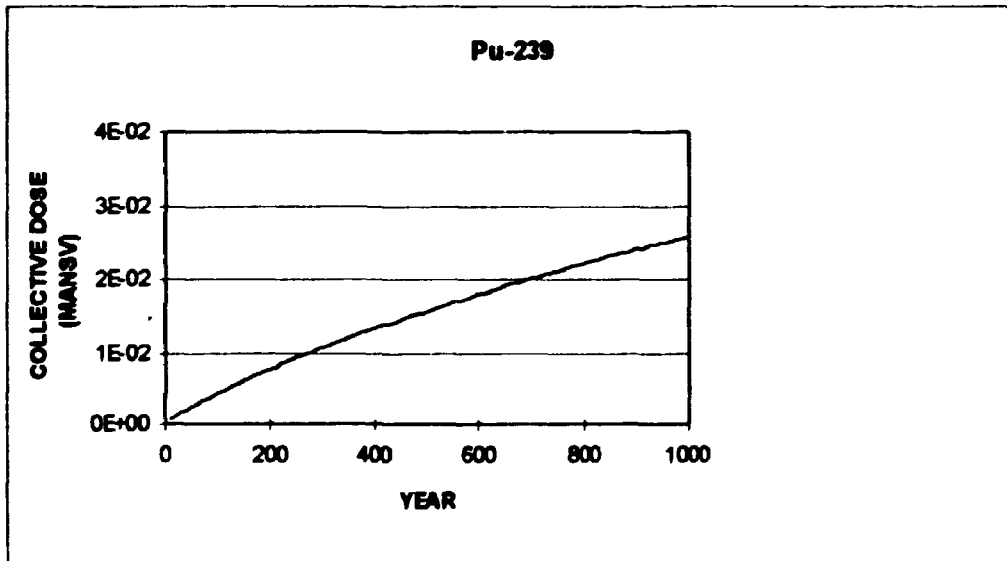
Figure B-6. Collective dose to the world population calculated from a single 1 TBq discharge of ^{60}Co in the Novaya Zemlya fjord at year zero.
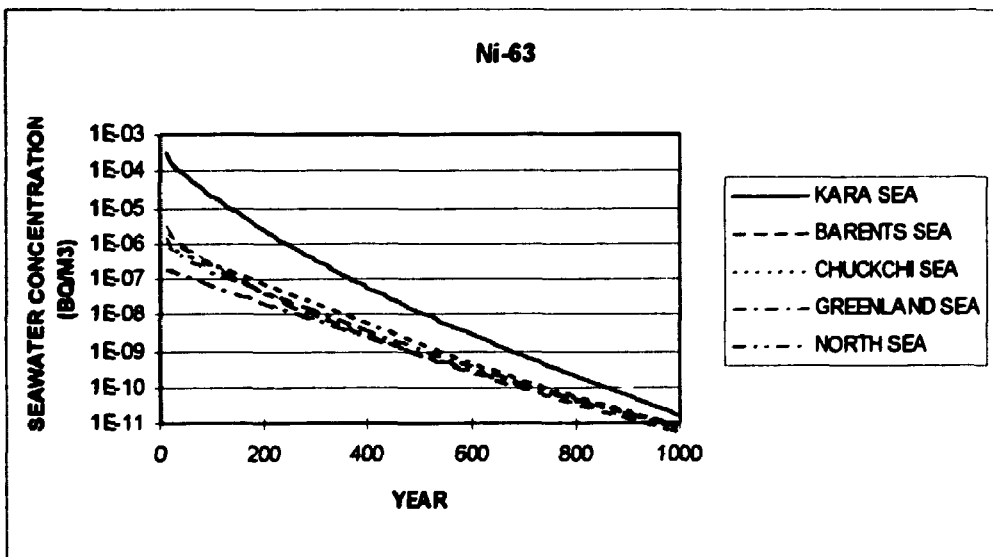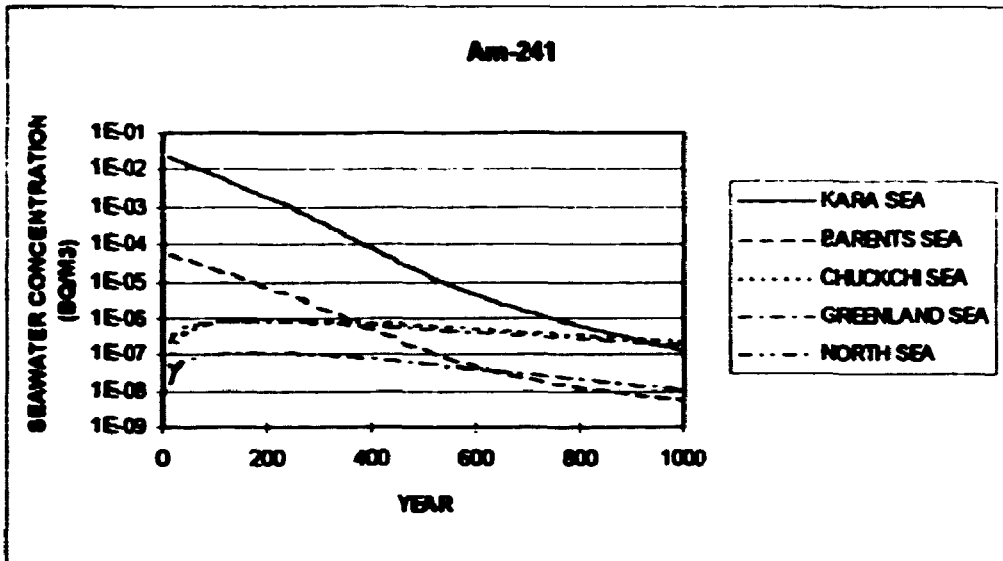

Figure B-7. Unfiltered seawater concentrations ($Bq\ m^{-3}$) in selected surface waters calculated from a single 1 TBq discharge of ^{63}Ni in the Novaya Zemlya fjord at year zero.
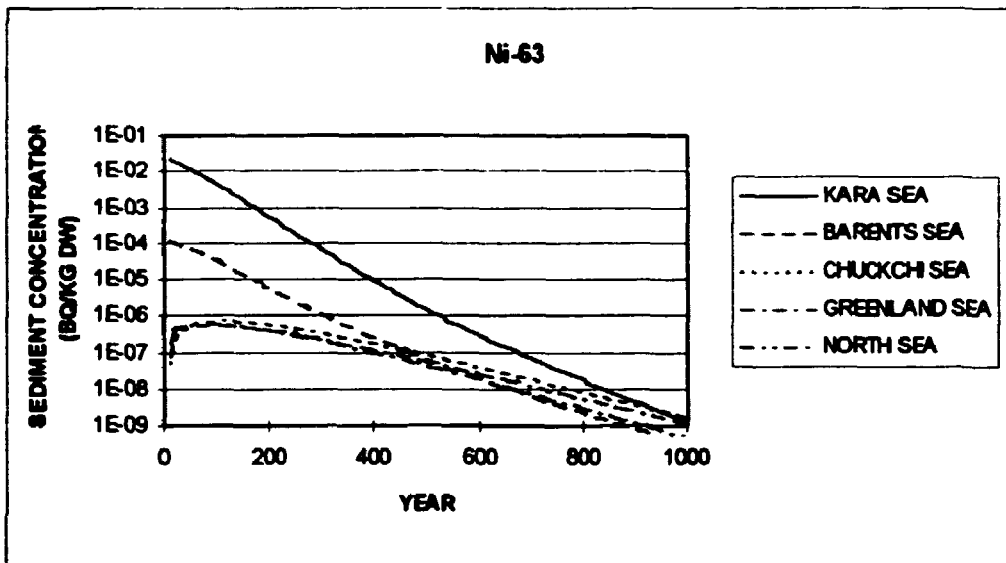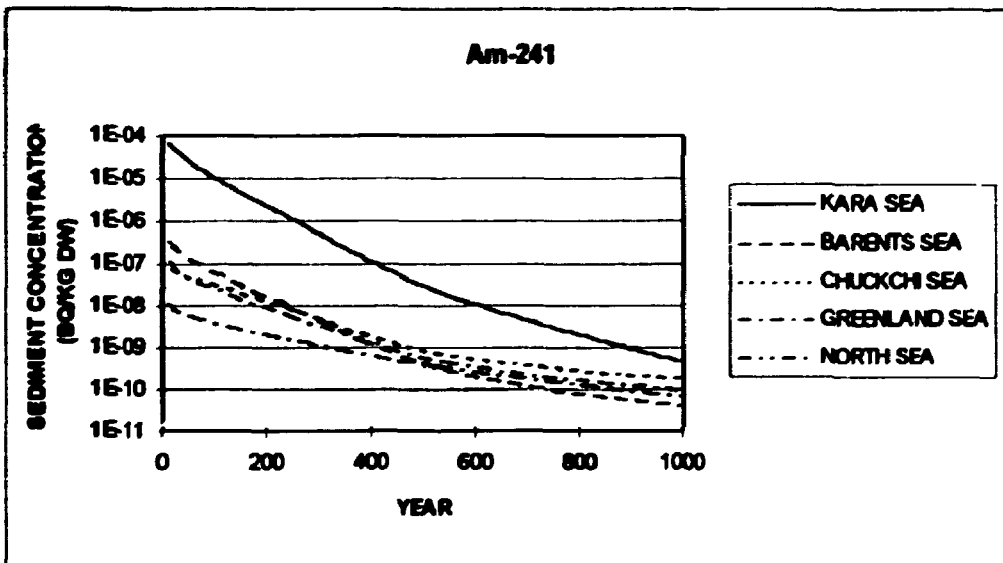
Figure B-8. Surface sediment concentrations (Bq kg^{-1} dw) in selected surface waters calculated from a single 1 TBq discharge of ^{63}Ni in the Novaya Zemlya fjord at year zero.
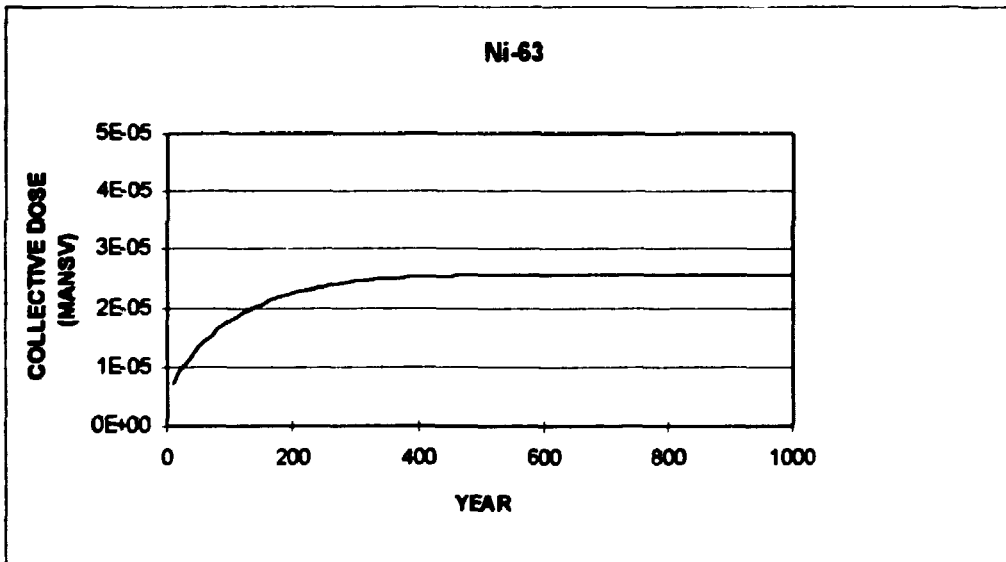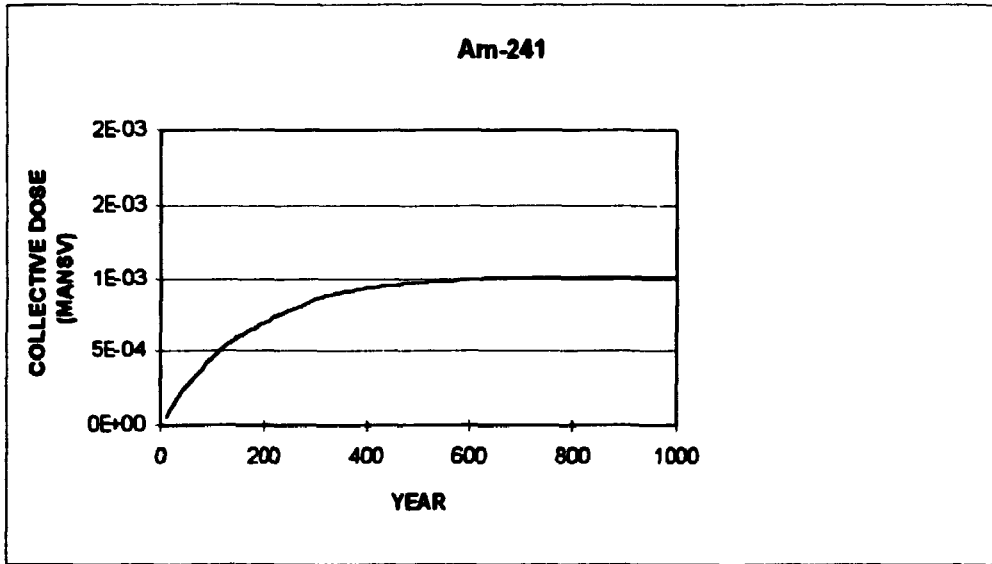

Figure B-9. Collective dose to the world population calculated from a single 1 TBq discharge of ^{63}Ni in the Novaya Zemlya fjord at year zero.
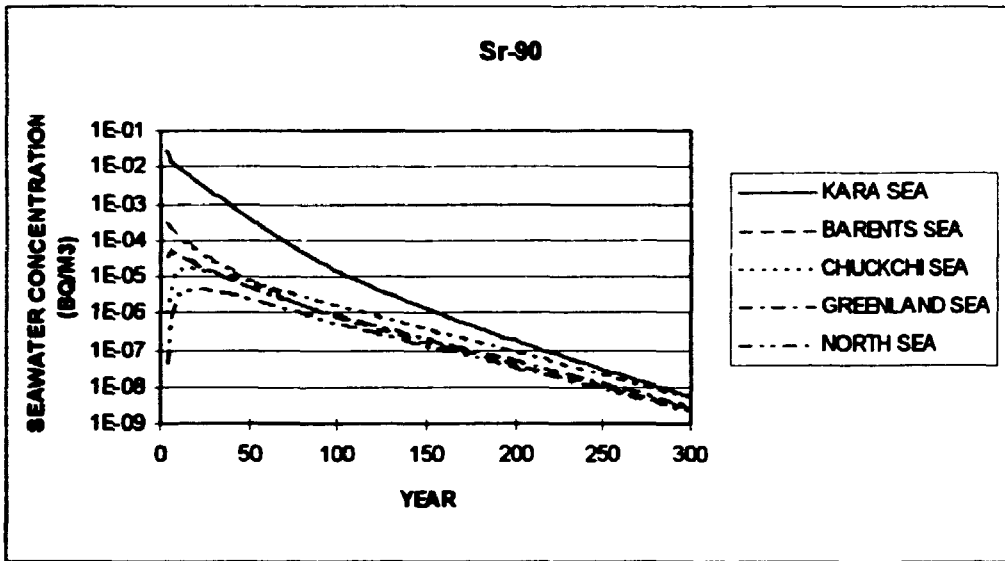
Figure B-10. Unfiltered seawater concentrations (Bq m⁻³) in selected surface waters calculated from a single 1 TBq discharge of ^{90}Sr in the Novaya Zemlya fjord at year zero.
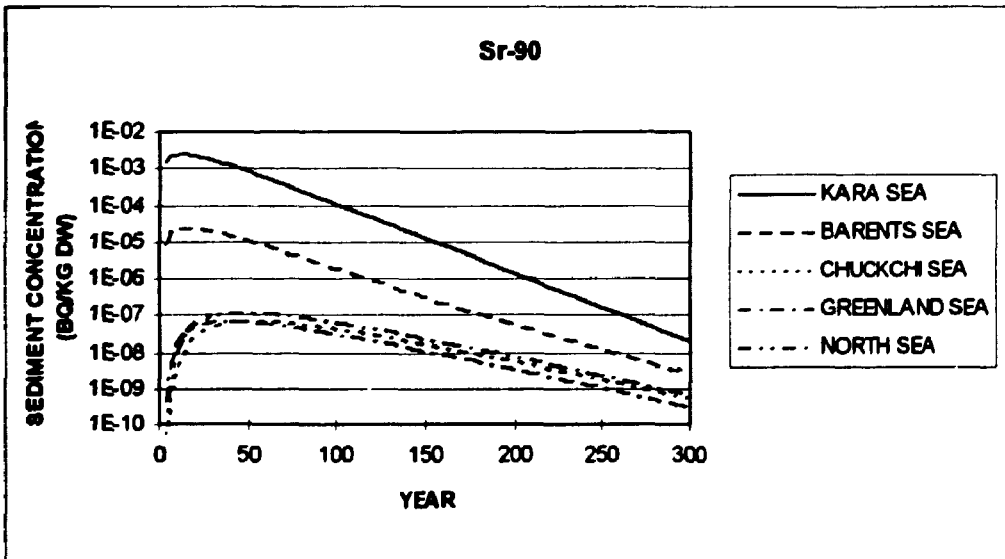
Figure B-11. Surface sediment concentrations (Bq kg⁻¹ dw) in selected surface waters calculated from a single 1 TBq discharge of ^{90}Sr in the Novaya Zemlya fjord at year zero.

Sr-90
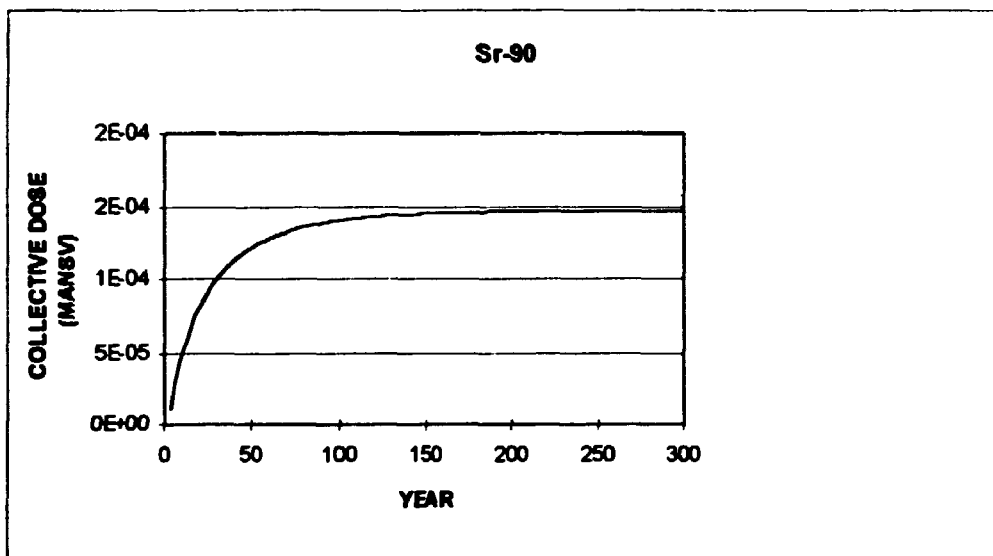
Figure B-12. Collective dose to the world population calculated from a single 1 TBq discharge of ^{90}Sr in the Novaya Zemlya fjord at year zero.

I-129

KARA SEA
BARENTS SEA
CHUCKCHI SEA
GREENLAND SEA
NORTH SEA
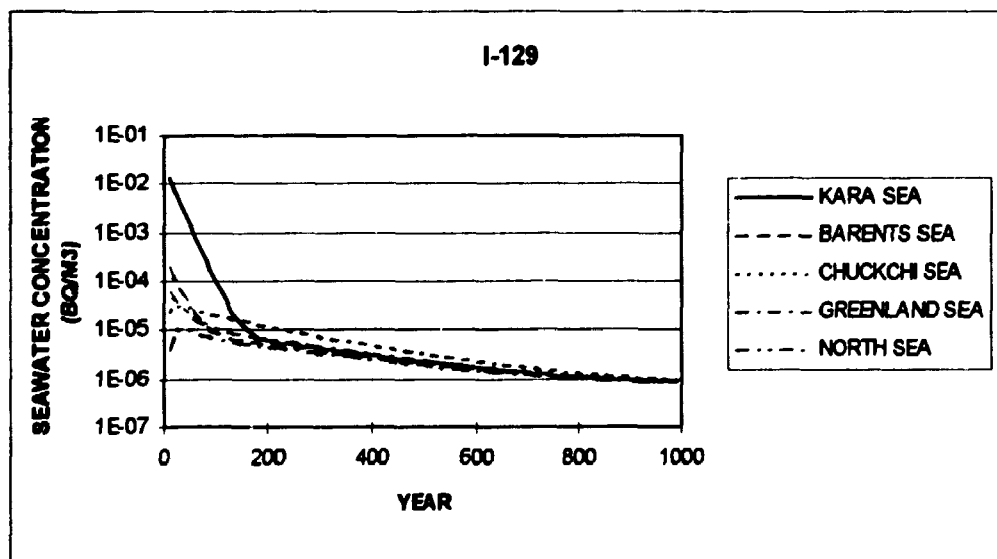
Figure B-13. Unfiltered seawater concentrations (Bq m^{-3}) in selected surface waters calculated from a single 1 TBq discharge of ^{129}I in the Novaya Zemlya fjord at year zero.

I-129
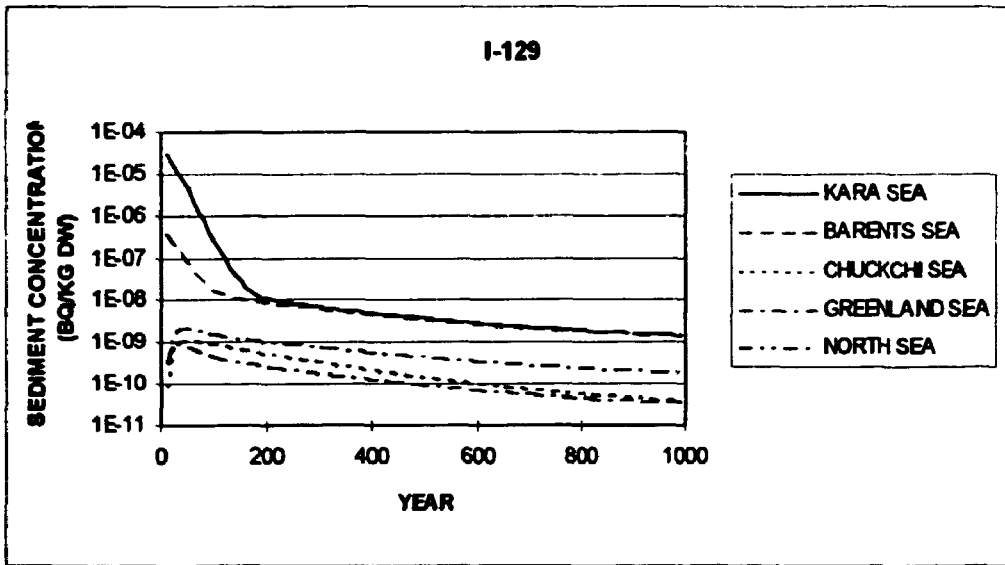
Figure B-14. Surface sediment concentrations (Bq kg^{-1} dw) in selected surface waters calculated from a single 1 TBq discharge of ^{129}I in the Novaya Zemlya fjord at year zero.

I-129
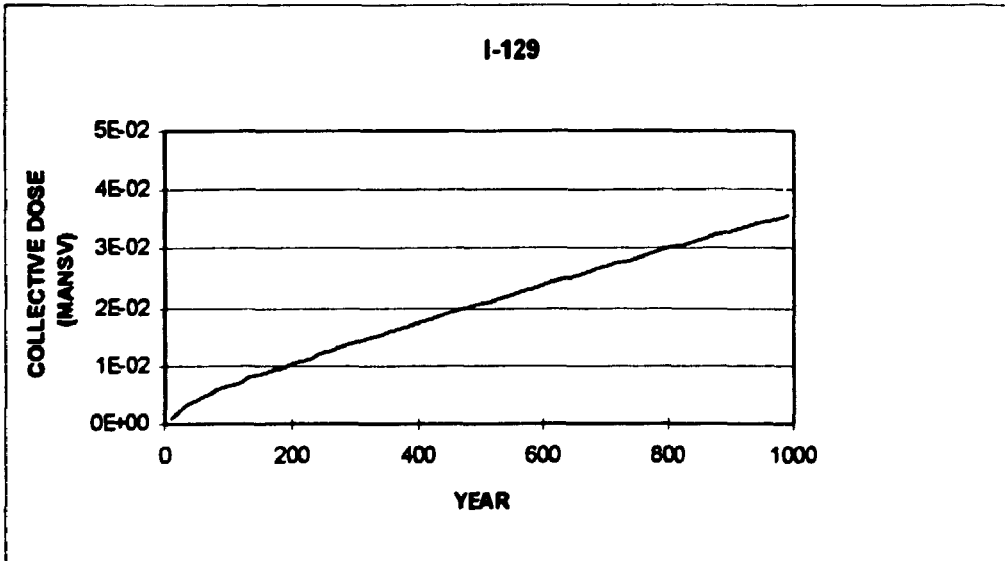
Figure B-15. Collective dose to the world population calculated from a single 1 TBq discharge of ^{129}I in the Novaya Zemlya fjord at year zero.
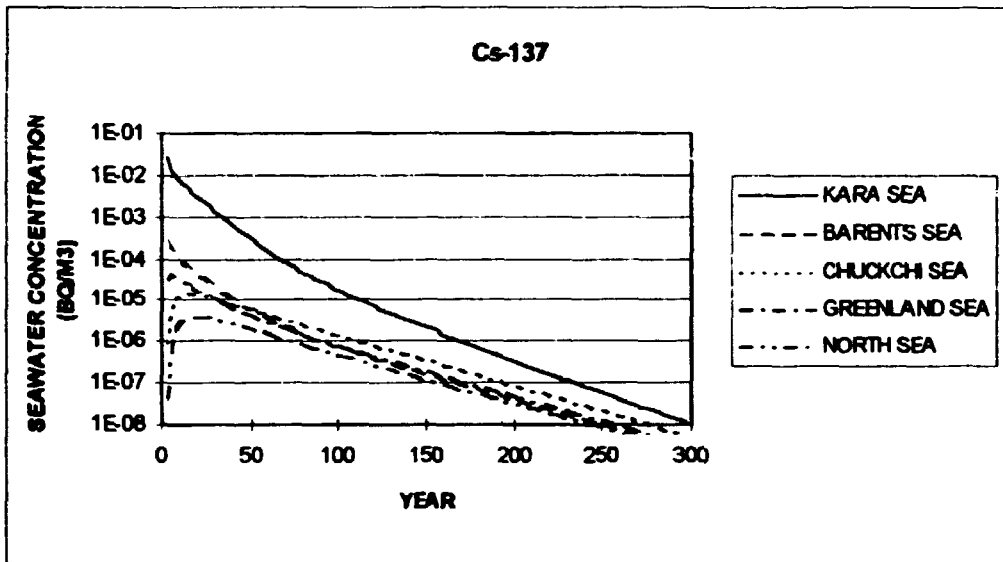
Figure B-16. Unfiltered seawater concentrations (Bq m^{-3}) in selected surface waters calculated from a single 1 TBq discharge of ^{137}Cs in the Novaya Zemlya fjord at year zero.

Figure B-17. Surface sediment concentrations (Bq kg^{-1} dw) in selected surface waters calculated from a single 1 TBq discharge of ^{137}Cs in the Novaya Zemlya fjord at year zero.

Cs-137

Figure B-18. Collective dose to the world population calculated from a single 1 TBq discharge of ^{137}Cs in the Novaya Zemlya fjord at year zero.

Pu-239

KARA SEA
BARENTS SEA
CHUCKCHI SEA
GREENLAND SEA
NORTH SEA

Figure B-19. Unfiltered seawater concentrations (Bq m^{-3}) in selected surface waters calculated from a single 1 TBq discharge of ^{239}Pu in the Novaya Zemlya fjord at year zero.

Figure B-20. Surface sediment concentrations (Bq kg^{-1} dw) in selected surface waters calculated from a single 1 TBq discharge of ^{239}Pu in the Novaya Zemlya fjord at year zero.

Figure B-21. Collective dose to the world population calculated from a single 1 TBq discharge of ^{239}Pu in the Novaya Zemlya fjord at year zero.

Figure B-22. Unfiltered seawater concentrations (Bq m^{-3}) in selected surface waters calculated from a single 1 TBq discharge of ^{241}Am in the Novaya Zemlya fjord at year zero.

Figure B-23. Surface sediment concentrations (Bq kg^{-1} dw) in selected surface waters calculated from a single 1 TBq discharge of ^{241}Am in the Novaya Zemlya fjord at year zero.

Figure B-24. Collective dose to the world population calculated from a single 1 TBq discharge of [241]Am in the Novaya Zemlya fjord at year zero.

10. APPENDIX C, Results of scenario releases

This appendix contains graphical presentations of selected results of the calculations of Scenario 1 (worst case) releases into the Arctic Seas. The results of unfiltered seawater concentrations, surface sediment concentrations and integrated collective doses are shown versus time. The graphs show the calculated seawater concentrations for the Western Kara Sea (box 1), the Southern Barents Sea (box 27), the Chuckchi Sea (box 13), the Greenland Sea (box 29) and the Central North Sea (box 107). The sediment concentrations are from the corresponding sediment boxes no. 2, 28, 15, 31 and 108. Furthermore, the collective dose to the world population calculated from ingestion of seafood is also shown versus time.
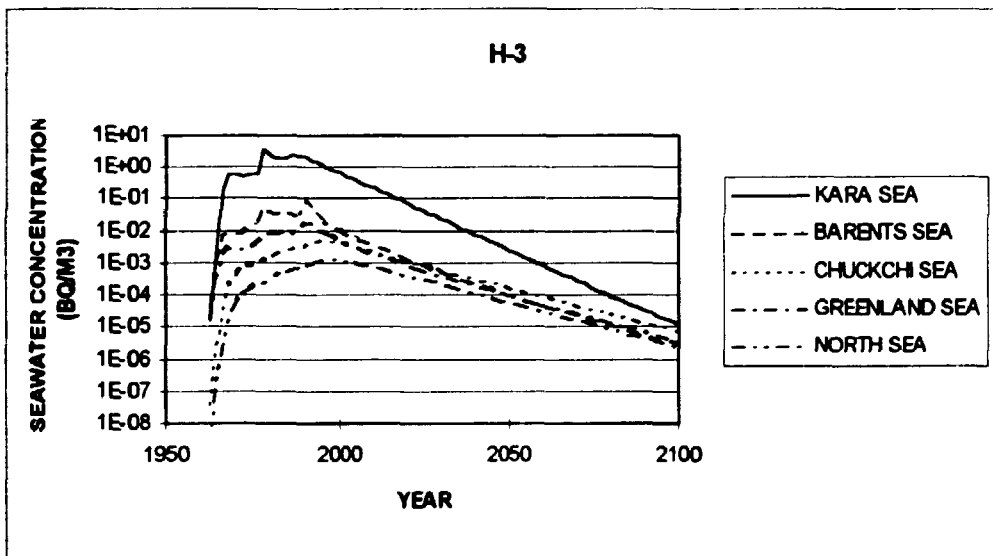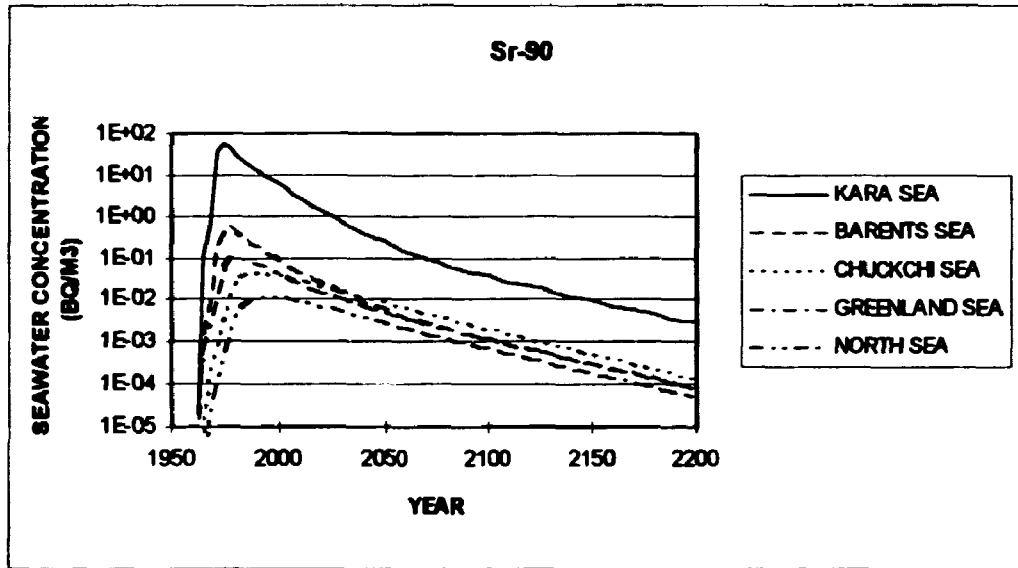

Figure C-1. Unfiltered seawater concentrations of ^3H (Bq m^{-3}) in surface waters from selected regions calculated as a function of time for release Scenario 1.
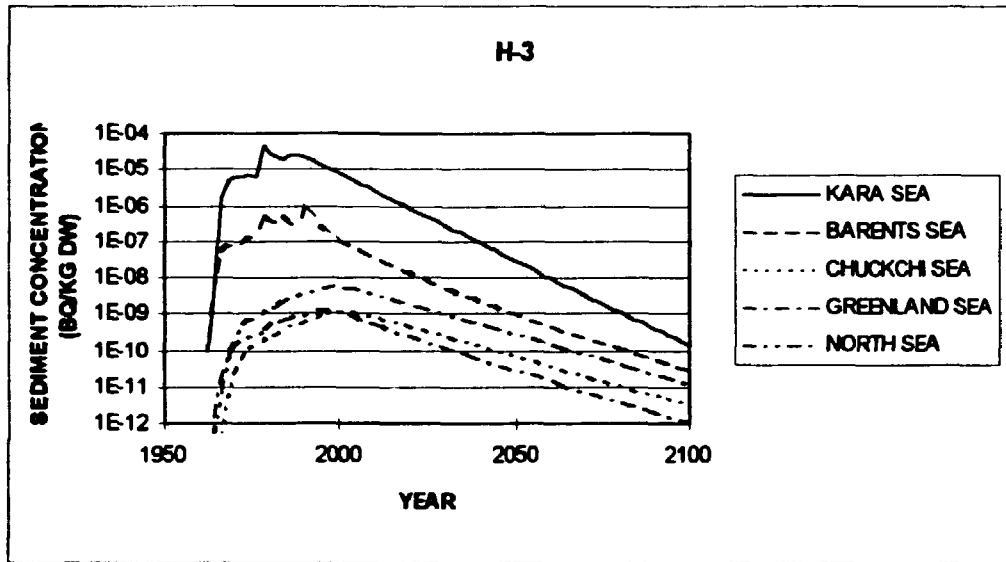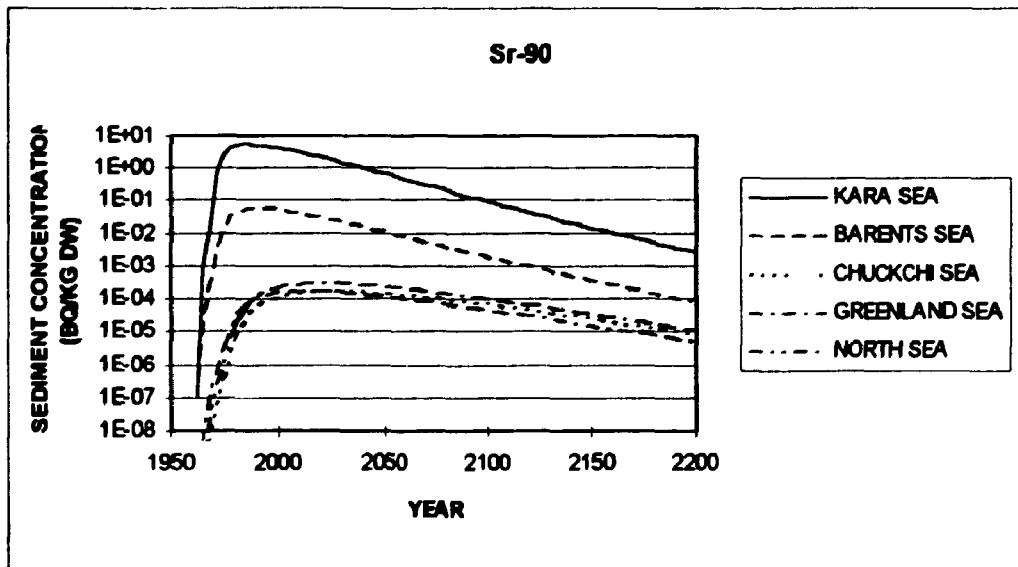
Figure C-2. Surface sediment concentrations of ^{3}H (Bq kg^{-1} dw) from selected regions calculated as a function of time for release Scenario 1.
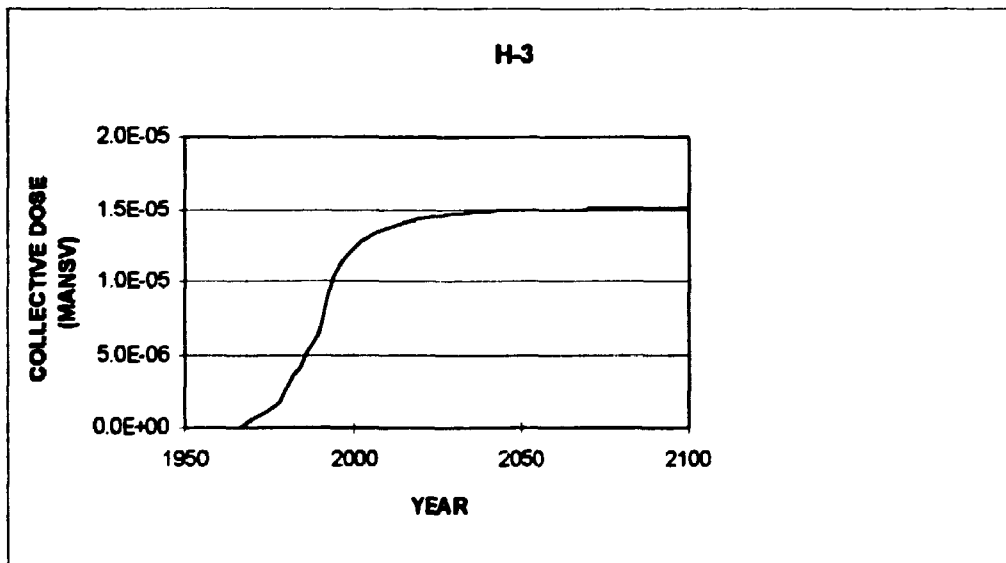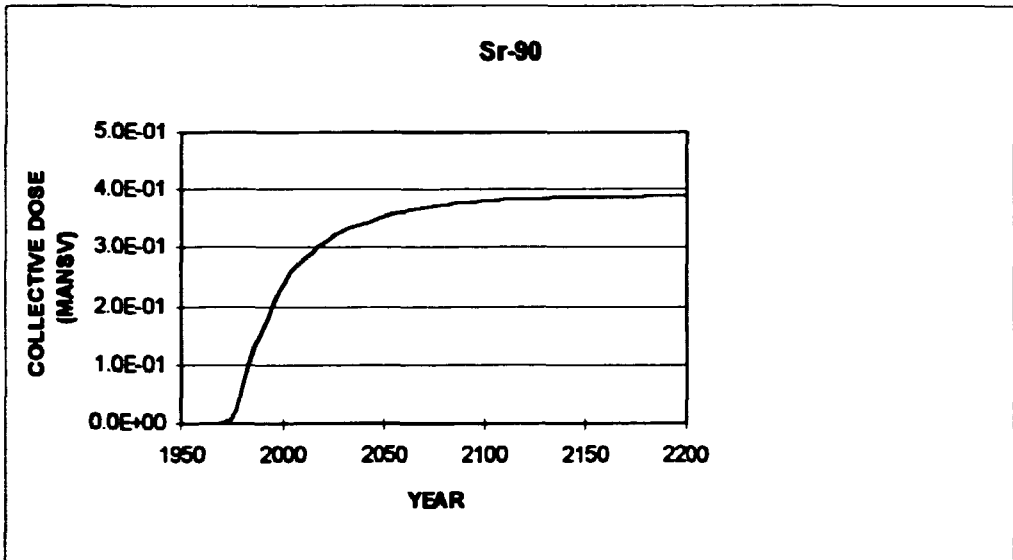

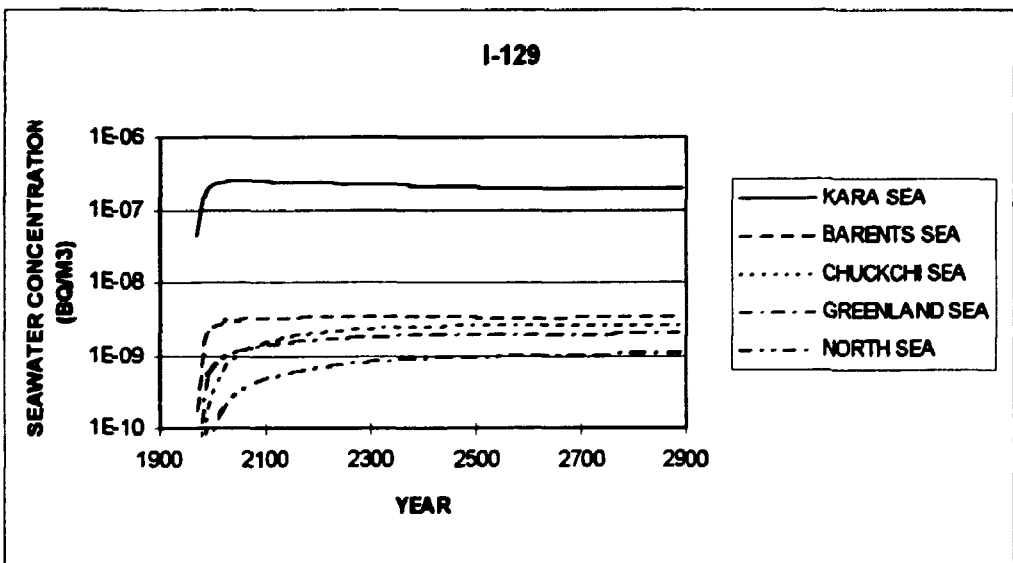**Figure C-3.** Collective dose to the world population from ^{3}H calculated for release Scenario 1.
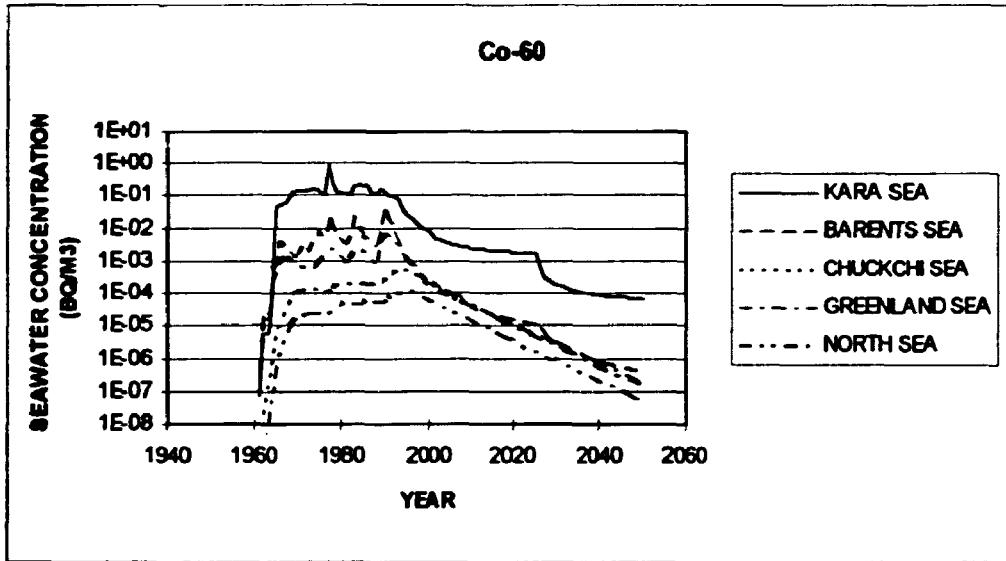
Figure C-4. Unfiltered seawater concentrations of ^{60}Co (Bq m^{-3}) in surface waters from selected regions calculated as a function of time for release Scenario 1.
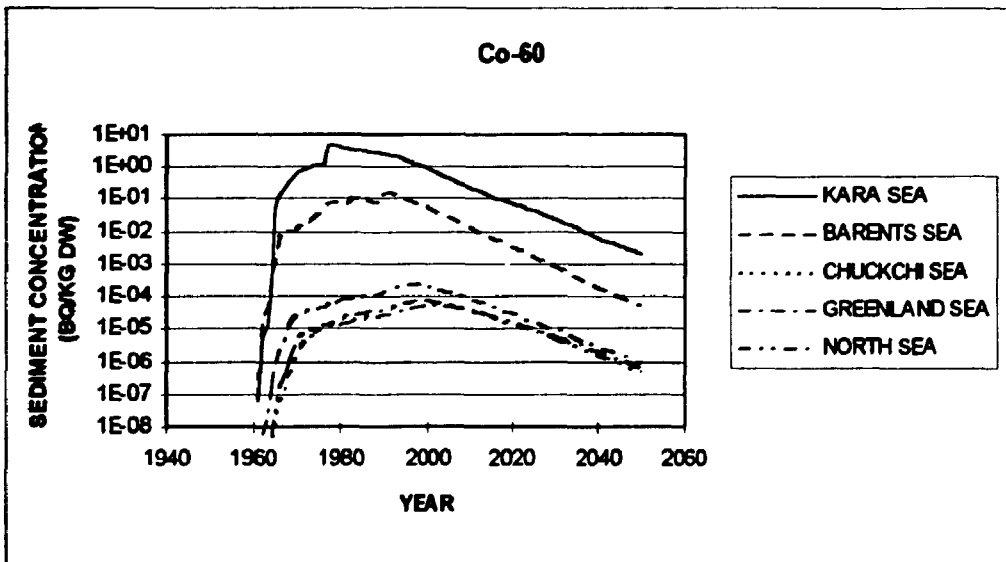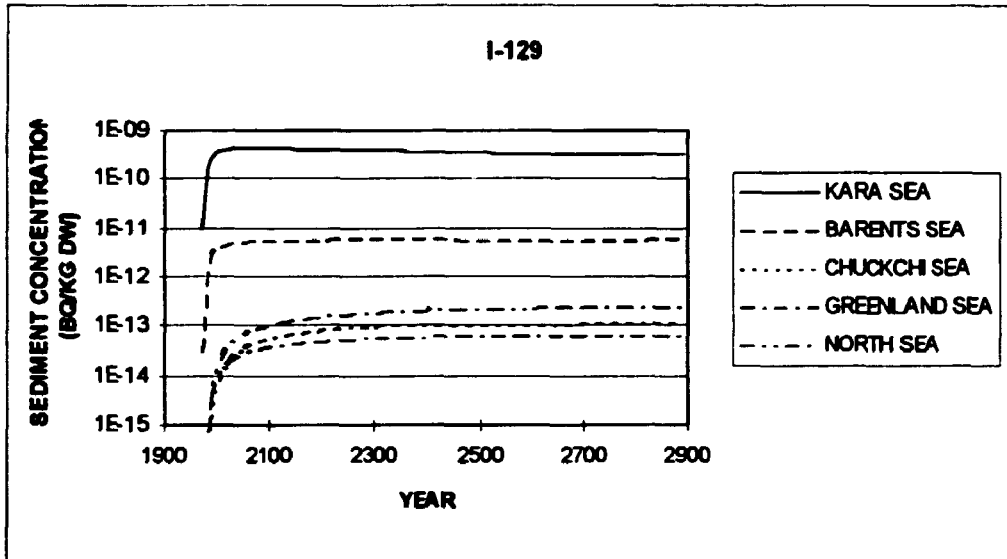

Figure C-5. Surface sediment concentrations of ^{60}Co (Bq kg^{-1} dw) from selected regions calculated as a function of time for release Scenario 1.
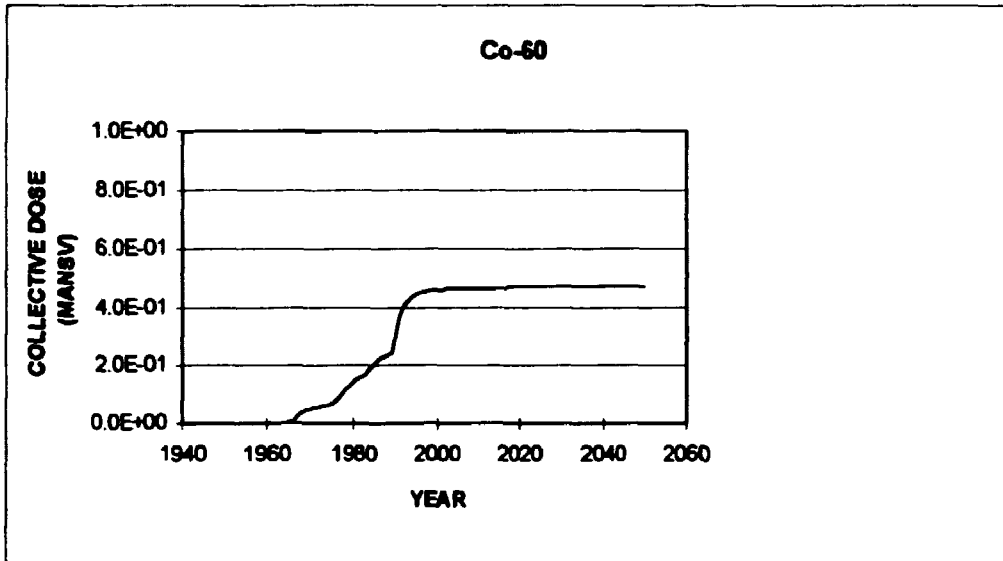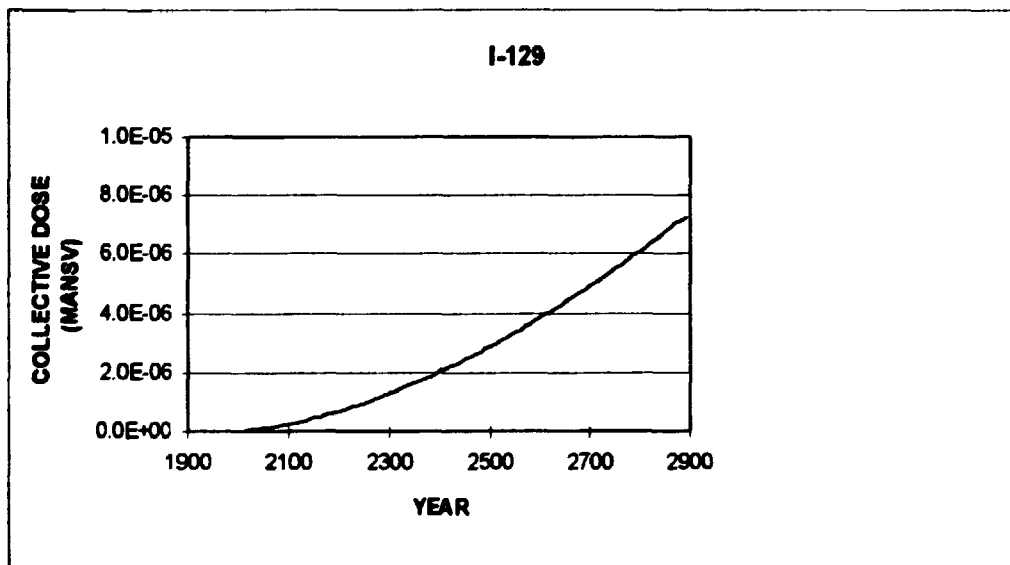
Figure C-6. Collective dose to the world population from ^{60}Co calculated for release Scenario 1.
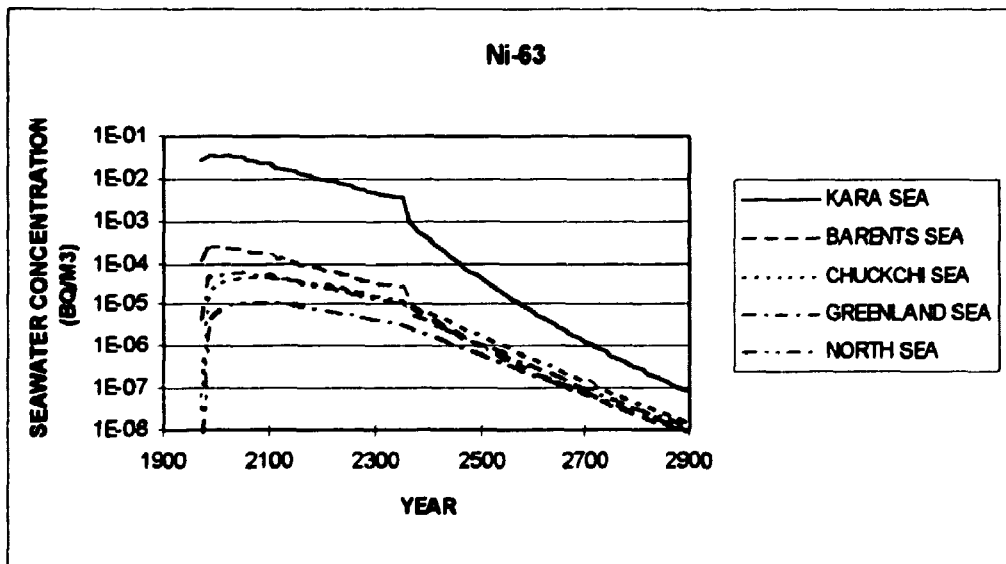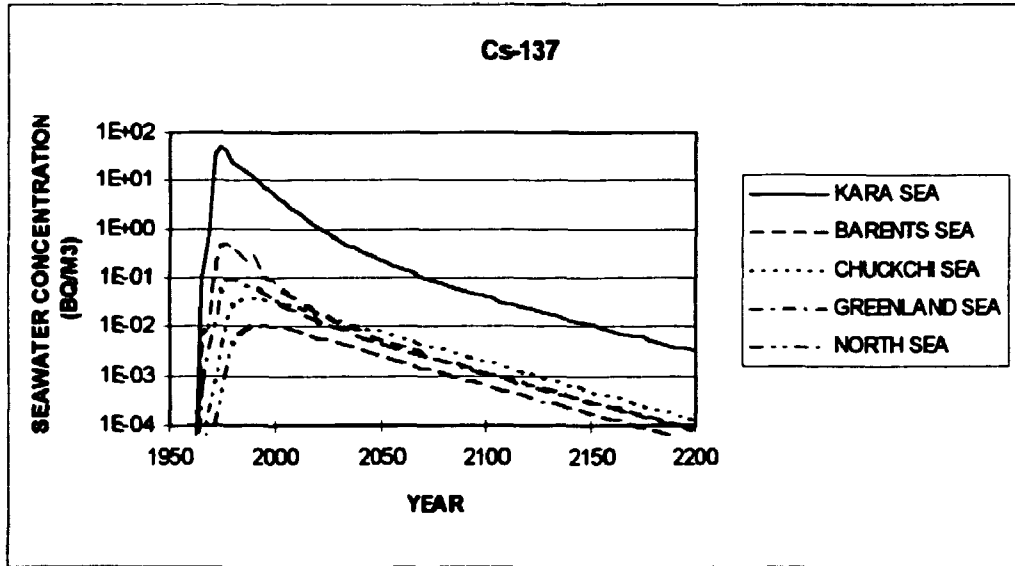

Figure C-7. Unfiltered seawater concentrations of ^{63}Ni (Bq m^{-3}) in surface waters from selected regions calculated as a function of time for release Scenario 1.
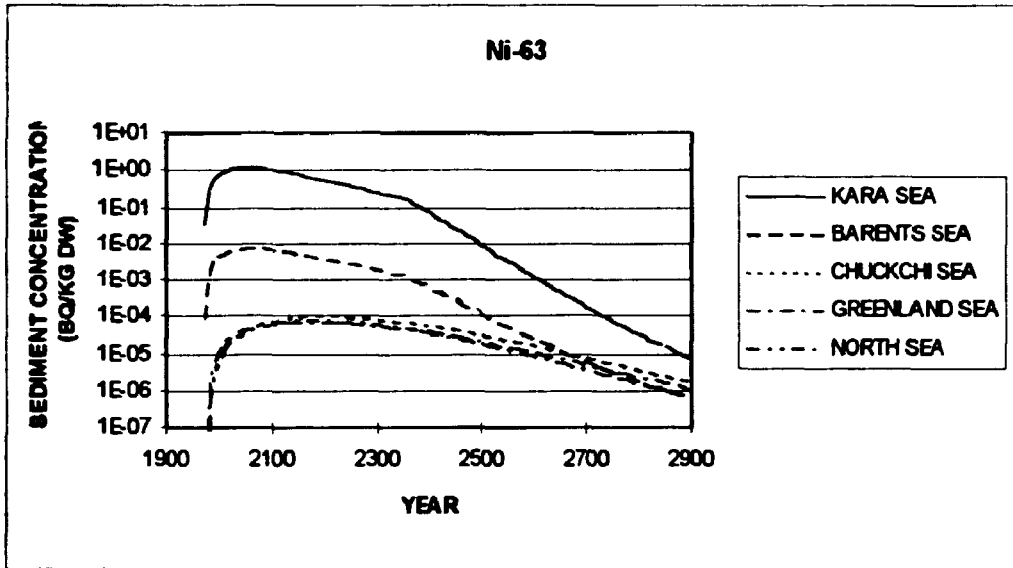
Figure C-8. Surface sediment concentrations of ^{63}Ni (Bq kg^{-1} dw) from selected regions calculated as a function of time for release Scenario 1.
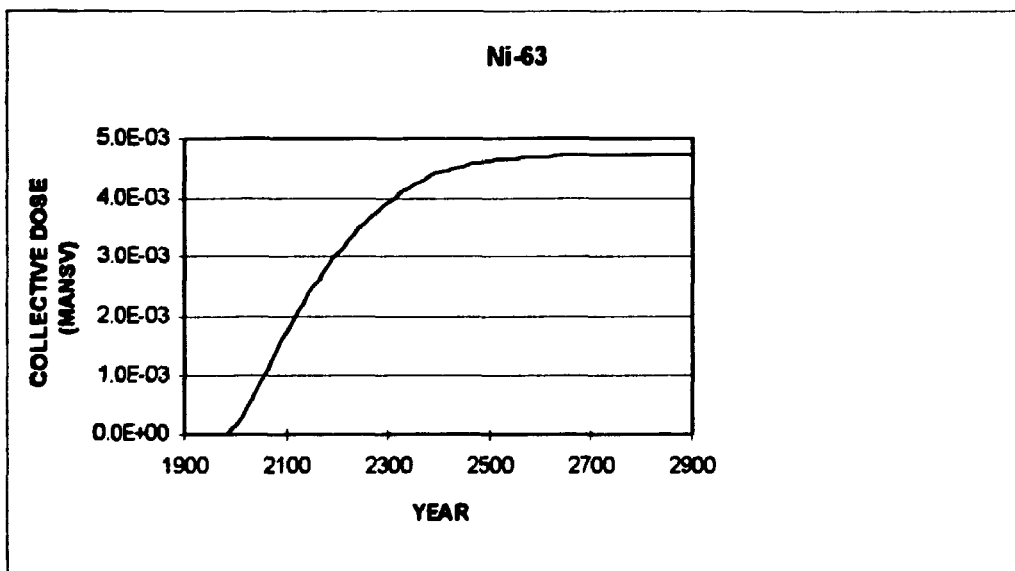
Figure C-9. Collective dose to the world population from ^{63}Ni calculated for release Scenario 1.

Figure C-10. Unfiltered seawater concentrations of ^{90}Sr (Bq m^{-3}) in surface waters from selected regions calculated as a function of time for release Scenario 1.
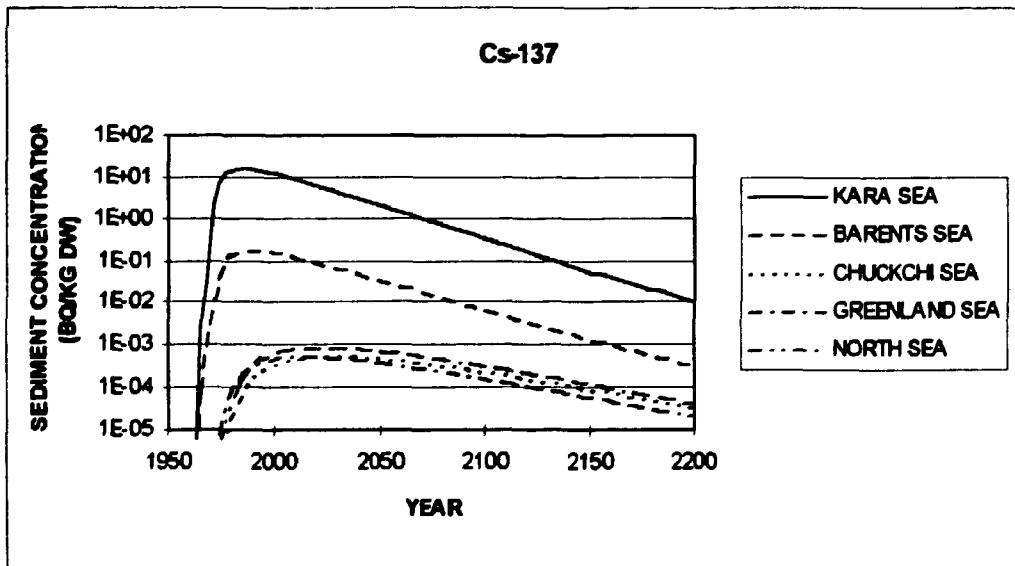

Figure C-11. Surface sediment concentrations of ^{90}Sr (Bq kg^{-1} dw) from selected regions calculated as a function of time for release Scenario 1.
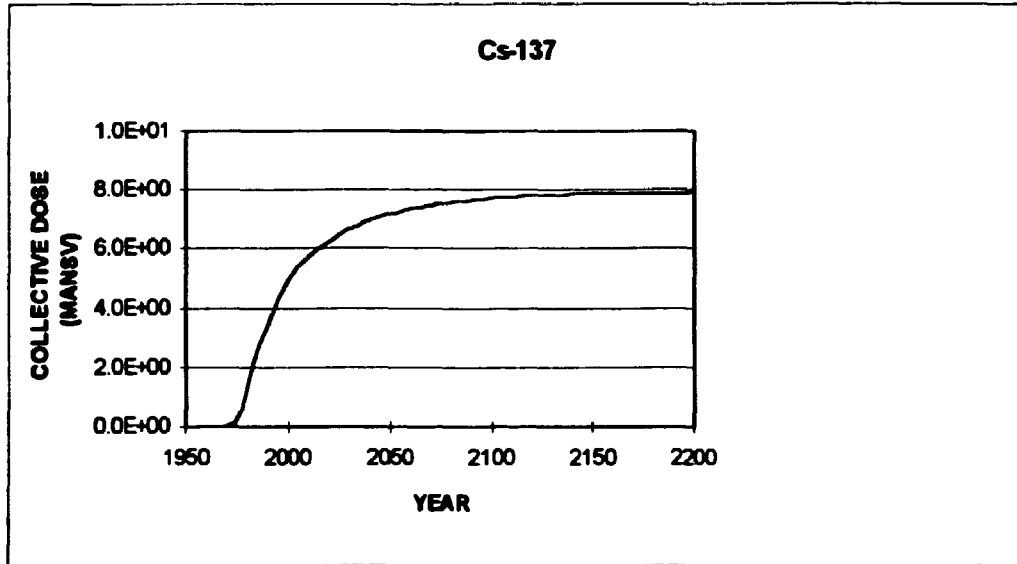
Figure C-12. Collective dose to the world population from ^{90}Sr calculated for release Scenario 1.
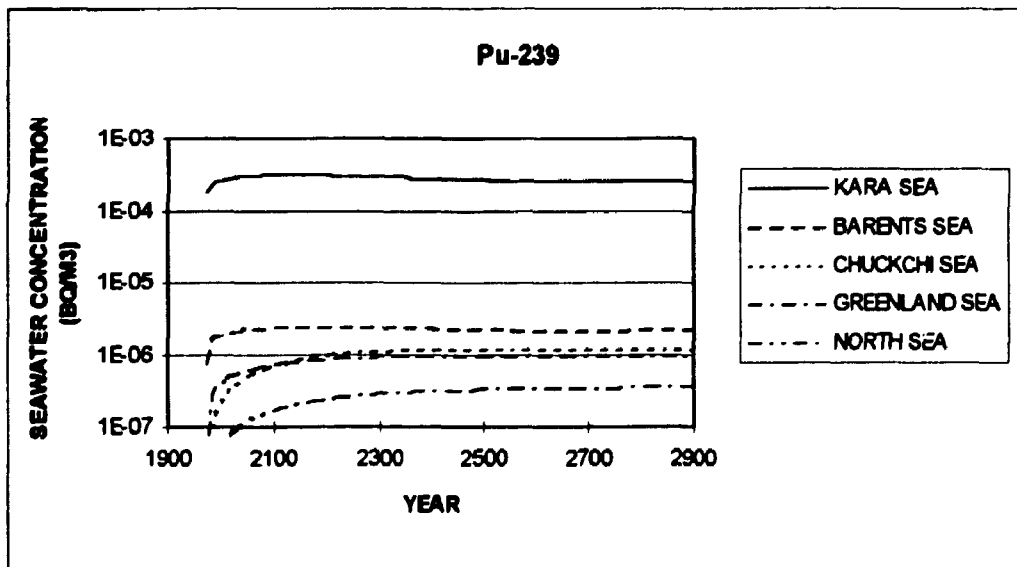

Figure C-13. Unfiltered seawater concentrations of ^{129}I (Bq m^{-3}) in surface waters from selected regions calculated as a function of time for release Scenario 1.

Figure C-14. Surface sediment concentrations of ^{129}I (Bq kg^{-1} dw) from selected regions calculated as a function of time for release Scenario 1.

Figure C-15. Collective dose to the world population from ^{129}I calculated for release Scenario 1.

Figure C-16. Unfiltered seawater concentrations of [137]Cs (Bq m[-3]) in surface waters from selected regions calculated as a function of time for release Scenario 1.
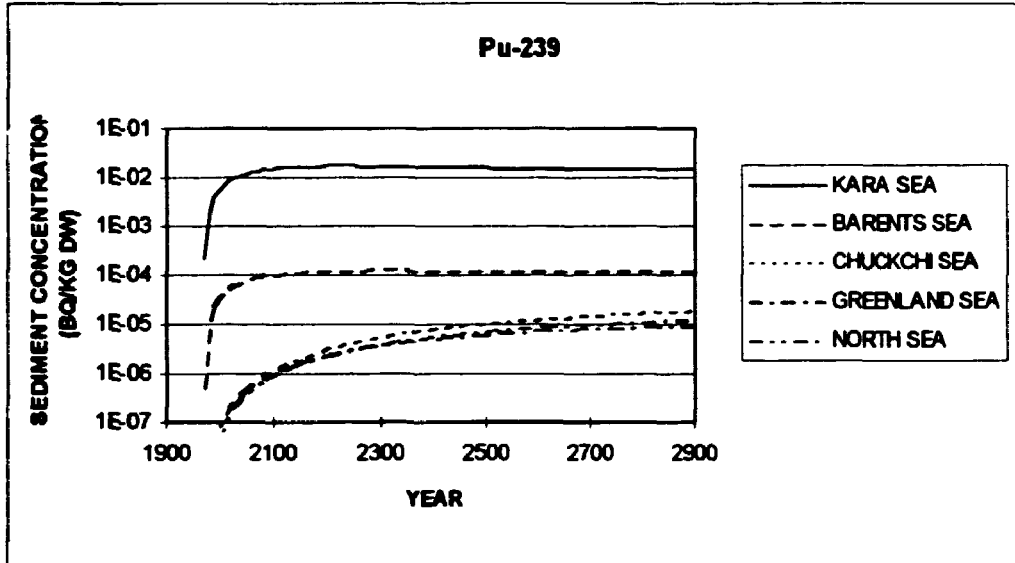

Figure C-17. Surface sediment concentrations of [137]Cs (Bq kg^{-1} dw) from selected regions calculated as a function of time for release Scenario 1.

Figure C-18. Collective dose to the world population from ^{137}Cs calculated for release Scenario 1.

Figure C-19. Unfiltered seawater concentrations of [239]Pu (Bq m^{-3}) in surface waters from selected regions calculated as a function of time for release Scenario 1.

Figure C-20. Surface sediment concentrations of ^{239}Pu (Bq kg^{-1} dw) from selected regions calculated as a function of time for release Scenario 1.
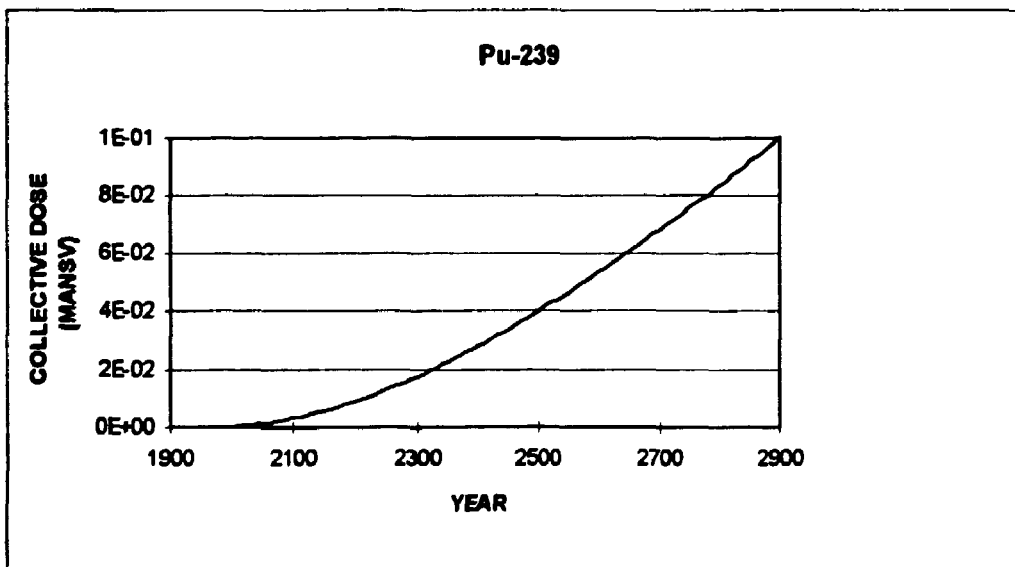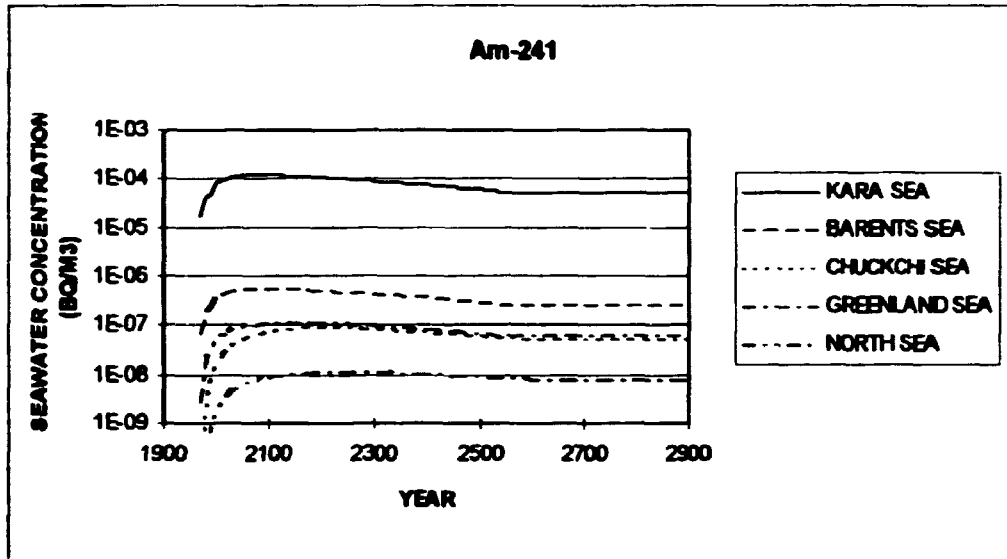

Figure C-21. Collective dose to the world population from ^{239}Pu calculated for release Scenario 1.

Figure C-22. Unfiltered seawater concentrations of ^{241}Am (Bq m^{-3}) in surface waters from selected regions calculated as a function of time for release Scenario 1.
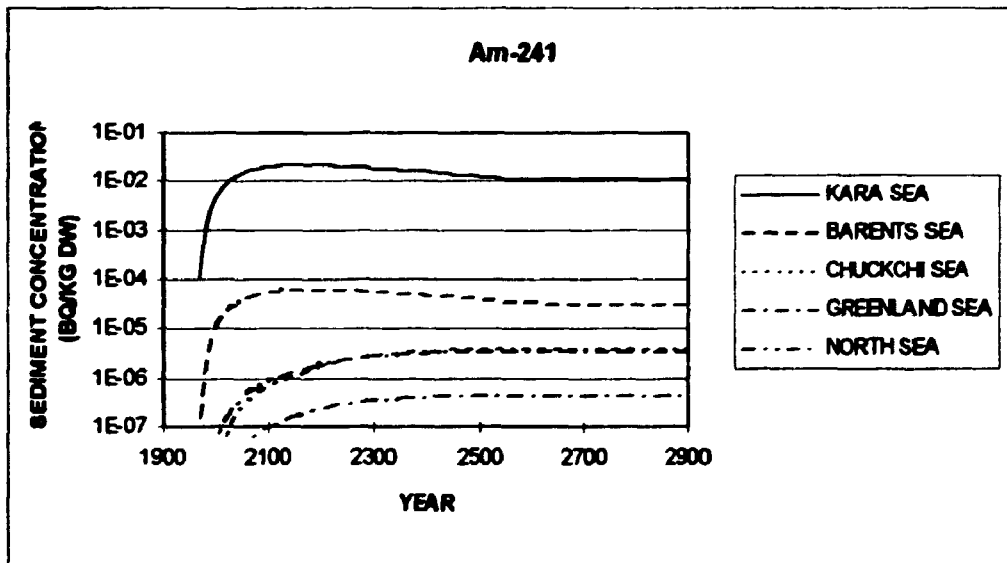

Figure C-23. Surface sediment concentrations of ^{241}Am (Bq kg^{-1} dw) from selected regions calculated as a function of time for release Scenario 1.
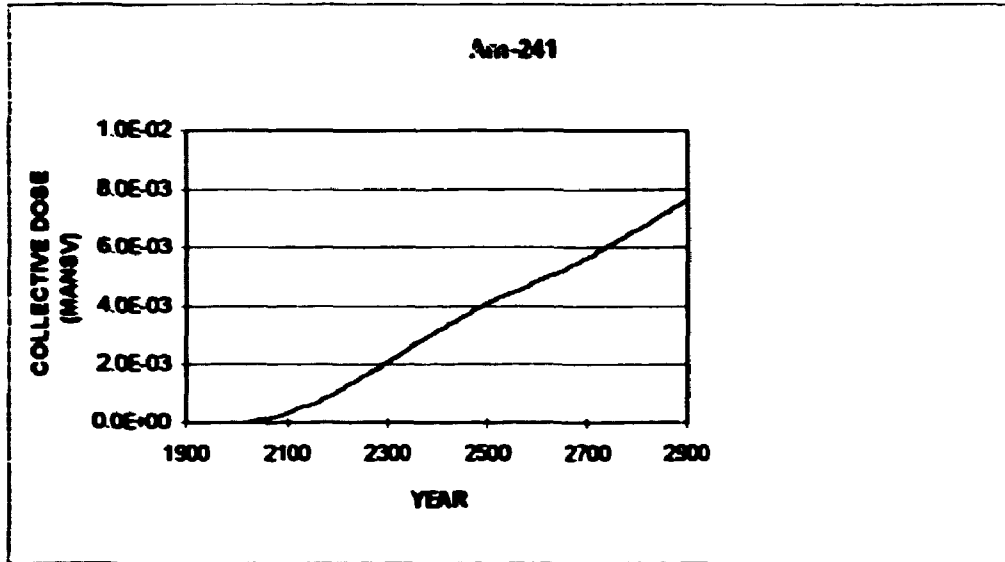
Figure C-24. Collective dose to the world population from [241]Am calculated for release Scenario 1.

Title and author(s)

A Preliminary Assessment of Potential Doses to Man from Radioactive Waste
Dumped in the Arctic Sea

Sven P. Nielsen, Mikhail Iosjpe and Per Strand

Abstract (Max. 2000 characters)

This report describes a preliminary radiological assessment of collective doses to the
world population from radioactive material dumped in the Barents and Kara Seas in the
period 1961-1991. Information on the dumped waste and the rates of release of
radionuclides have been available from Russian sources and from the International
Atomic Energy Agency. A box model has been used to simulate the dispersion of
radionuclides in the marine environment and to calculate the contamination of seafood
and the subsequent radiation doses to man. Two release scenarios have been adopted.
The worst-case release scenario which ignores the presence of barriers between spent
nuclear fuel and seawater is estimated to give rise to about 10 mansieverts calculated to
1000 years from the time of release. A more realistic release scenario is estimated to
cause about 3 mansieverts. In both cases exposure from the radionuclide ^{137}Cs is found
to dominate the doses.

Descriptors INIS/EDB

ARCTIC OCEAN; BOX MODELS; CESIUM 137; ENVIRONMENTAL
EFFECTS; FISSION PRODUCT RELEASE; FOOD CHAINS; HUMAN
POPULATIONS; MARINE DISPOSAL; NOVAYA ZEMLYA; RADIATION
DOSES; RADIOACTIVE WASTE DISPOSAL; SEAFOOD; SEAWATER;
SOURCE TERMS

RISØ

Objective

The objective of Risø's research is to provide industry and society with new potential in three main areas:

* *Energy technology and energy planning*
* *Environmental aspects of energy, industrial and plant production*
* *Materials and measuring techniques for industry*

As a special obligation Risø maintains and extends the knowledge required to advise the authorities on nuclear matters.

Research Profile

Risø's research is long-term and knowledge-oriented and directed toward areas where there are recognised needs for new solutions in Danish society. The programme areas are:

* *Combustion and gasification*
* *Wind energy*
* *Energy technologies for the future*
* *Energy planning*
* *Environmental aspects of energy and industrial production*
* *Environmental aspects of plant production*
* *Nuclear safety and radiation protection*
* *Materials with new physical and chemical properties*
* *Structural materials*
* *Optical measurement techniques and information processing*

Transfer of Knowledge

The results of Risø's research are transferred to industry and authorities through:

* *Research co-operation*
* *Co-operation in R&D consortia*
* *R&D clubs and exchange of researchers*
* *Centre for Advanced Technology*
* *Patenting and licencing activities*

To the scientific world through:

* *Publication activities*
* *Co-operation in national and international networks*
* *PhD- and Post Doc. education*

Key Figures

Risø has a staff of just over 900, of which more than 300 are scientists and 80 are PhD and Post Doc. students. Risø's 1995 budget totals DKK 476m, of which 45% come from research programmes and commercial contracts, while the remainder is covered by government appropriations.